FNP

JOURNAL OF FOOD PROCESS ENGINEERING

D.R. HELDMAN
and
R.P. SINGH
COEDITORS

FOOD & NUTRITION PRESS, INC.

VOLUME 14, NUMBER 1 QUARTERLY

JOURNAL OF FOOD PROCESS ENGINEERING

All articles for publication and inquiries regarding publication should be sent to DR. D.R. HELDMAN, COEDITOR, *Journal of Food Process Engineering,* National Food Processors Association, 1401 New York Ave., N.W., Washington, D.C. 20005 USA: or DR. R.P. SINGH, COEDITOR, *Journal of Food Process Engineering,* University of California, Davis, Department of Agricultural Engineering, Davis, CA 95616 USA.

All subscriptions and inquiries regarding subscriptions should be sent to Food & Nutrition Press, Inc., 6527 Main Street, P.O. Box 374, Trumbull, CT 06611 USA.

One volume of four issues will be published annually. The price for Volume 14 is $104.00 which includes postage to U.S., Canada, and Mexico. Subscriptions to other countries are $123.00 per year via surface mail, and $132.00 per year via airmail.

Subscriptions for individuals for their own personal use are $84.00 for Volume 14 which includes postage to U.S., Canada, and Mexico. Personal subscriptions to other countries are $103.00 per year via surface mail, and $112.00 per year via airmail. Subscriptions for individuals should be sent direct to the publisher and marked for personal use.

The *Journal of Food Process Engineering* (ISSN: 0145-8876) is published quarterly (March, June, September and December) by Food & Nutrition Press, Inc.—Office of Publication is 6527 Main Street, P.O. Box 374, Trumbull, Connecticut 06611 USA. (Current issue is May 1991.)

Second class postage paid at Bridgeport, CT 06602.

POSTMASTER: Send address changes to Food & Nutrition Press, Inc., 6527 Main Street, P.O. Box 374, Trumbull, CT 06611.

JOURNAL OF FOOD PROCESS ENGINEERING

JOURNAL OF FOOD PROCESS ENGINEERING

Journal of FOOD PROCESS ENGINEERING

VOLUME 14
NUMBER 1

Coeditors: D.R. HELDMAN
R.P. SINGH

FOOD & NUTRITION PRESS, INC.
TRUMBULL, CONNECTICUT 06611 USA

ISSN 0145-8876

Printed in the United States of America

CONTENTS

ELASTIC MODULUS OF ORANGE JUICE ICE

HISAHIKO WATANABE[1], YOSHIO HAGURA, MASANOBU ISHIKAWA, TOMOO MIHORI and YOSHIO SAKAI

Department of Food Science and Technology, Tokyo University of Fisheries, 4-5-7, Konan, Minato, Tokyo, 108 Japan

Accepted for Publication February 1, 1991

ABSTRACT

The elastic modulus of orange juice ice as well as pure water ice was measured at temperatures between −10°C and −196°C by compression tests. The elastic modulus of pure water ice was almost constant in the whole range of the tested temperatures: 5.6 × 10^9 N/m² at −196°C and 4.0 × 10^9 N/m² at −10°C. In contrast, the elastic modulus of orange juice ice changed greatly with temperature: 11 × 10^9 N/m² at −196°C and 0.2 × 10^9 N/m² at −10°C. Orange juice ice was considered to consist of pure water ice particles which are dispersed in a matrix of concentrated amorphous solution (CAS). The elastic modulus of CAS was calculated using an equation for a disperse system.

INTRODUCTION

Cryo-grinding of foodstuffs into fine powders is expected to become an innovative technique for preparing foodstuffs with high quality (Hagihara 1982). Another application of cryo-comminution is cryo-mechanical separation of agglomerated granules into individual units. Watanabe *et al.* (1987) studied the effect of temperature on the cryo-mechanical separation of citrus fruit into individual juice sacs.

There has not been much published data on mechanical properties, such as elastic modulus, tensile strength, and compressive strength for frozen foods, which are required for the design of cryo-comminution. In the present work, compression tests were used to obtain the elastic modulus of orange juice ice as well as of pure water ice at temperatures between −10°C and −196°C.

[1]Correspondence should be sent to: Hisahiko Watanabe, Dept. Food Sci. & Technol., Tokyo Univ. of Fisheries, 4-5-7, Konan, Minato, Tokyo, 108 Japan.

Journal of Food Process Engineering **14** (1991) 1–8. *All Rights Reserved.*

MATERIALS AND METHODS

Materials

Orange juice ice and pure water ice were prepared by the following process: The juice squeezed from sweet orange (*C. sinensis*) was filtered through two layers of cotton gauze. Distilled water was boiled to degas. The bottoms of aluminum tubes (2.0 cm i.d. × 2.0 cm) were covered with polyethylene film. The tubes were filled with orange juice or with degassed water. Tubes were covered with polyethylene film and placed in an air blast freezer at −20°C for twelve hours. After the samples froze, excess ice was removed from where it expanded outside of tubes by melting each end against a flat steel plate.

The ice blocks removed from tubes were used as test pieces. The test pieces were cooled to temperatures ranging from −10°C to −110°C in an air blast freezer, from −110°C to −170°C in low temperature gas evaporated from liquid nitrogen, and to −196°C in liquid nitrogen.

Apparatus

The testing machine was a UTM-4-200, Toyo Boldwin Co. (Fig. 1). The test piece supported on the bearing block, F, was suspended in a Dewar vessel, D. The environment in the vessel was kept at a preset temperature by controlling the evaporation rate of liquid nitrogen, K. The rate was regulated with the heater, L, under liquid. The test piece was compressed between the bearing blocks E and F. Bearing block E was connected to the cross head, C, which moved downwards at a constant speed, 5.0 mm/min, driven by screws, B. Bearing block F was fixed to the frame of the machine through an electronic load cell, A (Model TM-100 L, Toyo Boldwin Co.), by which the applied force was measured. The strain was measured by a digital strain meter, H (Model S332, Onosokki Co.).

RESULTS AND DISCUSSION

The elastic moduli of orange juice ice and pure water ice were determined at various temperatures ranging from −10°C to −196°C.

Elastic Modulus of Pure Water Ice

The stress-strain dependence of pure water ice showed that the stress first rose linearly until the sample broke. The slope of this straight line gave the elastic modulus comparable to published values (Gold 1977).

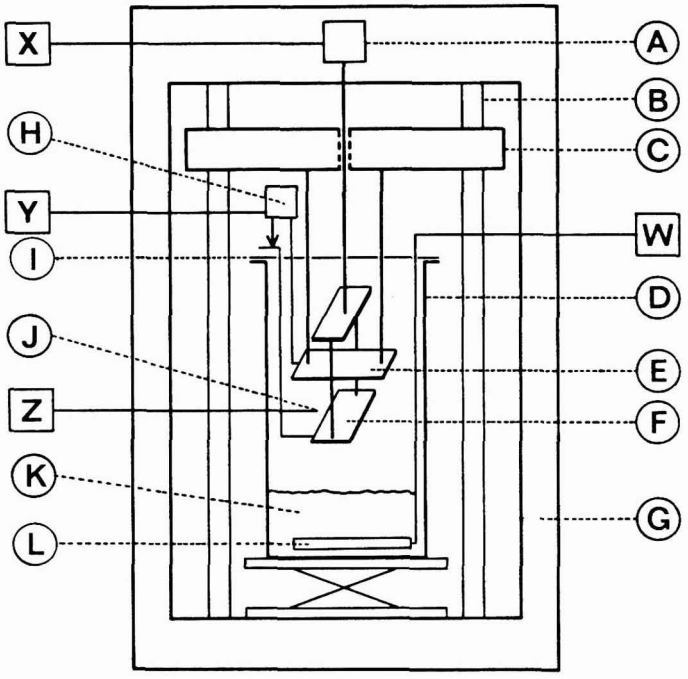

FIG. 1. A SCHEMATIC DIAGRAM OF EXPERIMENTAL APPARATUS
A: Load cell B: Screw, C: Cross head, D:Dewar vessel,
E: Bearing block (movable), F: Bearing block (fixed), G: Frame of machine,
H: Strain meter, I: Cover, J: Thermocouple, K: Liquid nitrogen
L: Heater, W: Regulator, X: Recorder for stress,
Y: Recorder for strain, Z: Thermometer.

Elastic Modulus of Orange Juice Ice

Two typical stress-strain diagrams of orange juice ice are shown in Fig. 2. At low temperature, a sudden breakage was observed, while at high temperature a gradual deformation took place. For small deformations, the stress-strain curves approached straight lines. The slopes of such straight lines gave the elastic moduli illustrated in Fig. 3. The elastic modulus of pure water ice was almost constant over the whole range of tested temperatures: 5.6×10^9 N/m^2 at -196°C and 4.0×10^9 N/m^2 at -10°C. The elastic modulus of orange juice ice, however, changed greatly with temperature: 11×10^9 N/m^2 at -196°C and 0.2×10^9 N/m^2 at -10°C.

It has been known that the elastic moduli of pure materials generally decrease very gradually with increase of temperature and retain finite values close to their melting points (DiBenedetto 1967). The behavior of the elastic modulus of pure

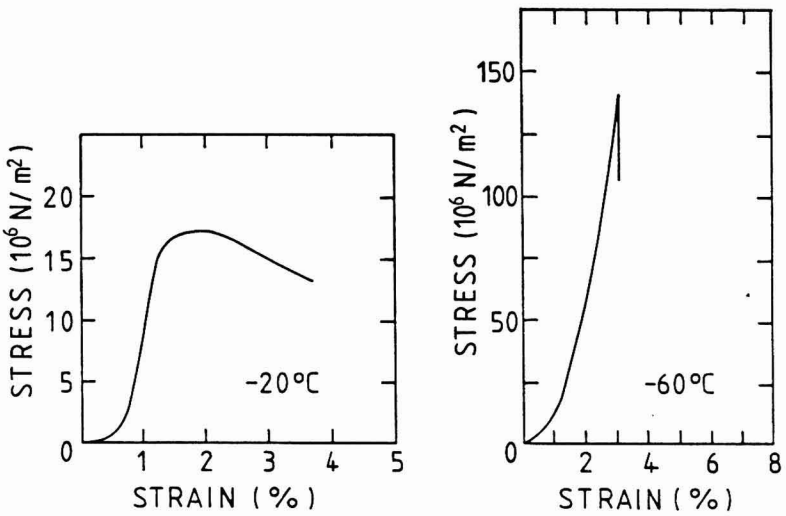

FIG. 2. TYPICAL STRESS-STRAIN DIAGRAMS OF ORANGE JUICE ICE

water ice agreed well with this observation. On the other hand, the modulus of orange juice ice showed a considerably steeper decrease from -150°C to -10°C as shown in Fig. 3. Such decrease arises from the fact that orange juice ice is not a pure material but a composite material consisting of pure water ice particles which are dispersed in the matrix of concentrated amorphous solution (CAS; Bellows and King 1972), as illustrated in Fig. 4.

Elastic Modulus of CAS

The elastic modulus of such a disperse composite system is given by Eq. (1) (Hansen 1965):

$$E_c = \frac{V_m E_m (2/3 + E_d/(3E_m)) + V_d E_d}{V_m(2/3 + E_d/(3E_m)) + V_d} \tag{1}$$

where E is elastic modulus, V is volume fraction, and the subscripts c, m, and d refer to composite, matrix and filler, respectively. When we substituted the elastic modulus of orange juice ice, E_j, and that of pure water ice E_{pw}, recorded in Fig. 3, for E_c and E_d and the volume fractions of pure water ice and CAS, V_{pw} and V_{CAS} for V_d and V_m, and solved Eq. (1) for the unknown E_m, we obtained elastic modulus of CAS, E_{CAS}.

The volume fractions V_{pw} and V_{CAS} in orange juice ice are given by:

$$V_{pw} = \frac{(1-s)I/\rho_{pw}}{((1-s)(1-I)+s)/\rho_{CAS} + (1-s)I/\rho_{pw}} \tag{2}$$

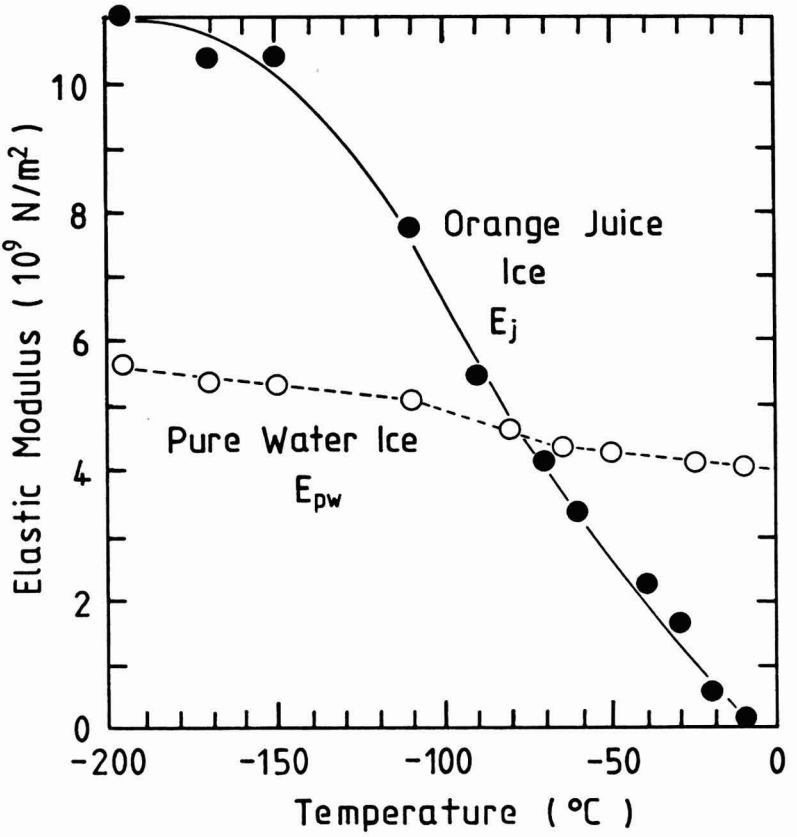

FIG. 3. ELASTIC MODULUS OF ORANGE JUICE ICE AND OF PURE WATER ICE AT TEMPERATURES BETWEEN −196°C AND −10°C

$$V_{CAS} = 1 - V_{pw} \tag{3}$$

where I is ice content of orange juice ice, s is solid content of original orange juice, ρ_{pw} is density of pure water ice, and ρ_{CAS} is density of CAS. Ice content was calculated by the method described by Chen (1985). We used −40°C as the eutectic point of orange juice (Chen 1985). The solid content of orange juice was taken as 11 wt % (Chen 1985). The density of pure water ice was assumed to be 0.920 g/ml (Lonsdale 1958). The density of an aqueous solution of sucrose (Synowietz 1977) was used in place of that of CAS, because sugar is the main soluble solid of orange juice.

The elastic moduli of CAS, E_{CAS}, thus obtained are shown in Fig. 5. When CAS is deeply cooled to temperatures below −150°C, E_{CAS} is larger than E_{pw}

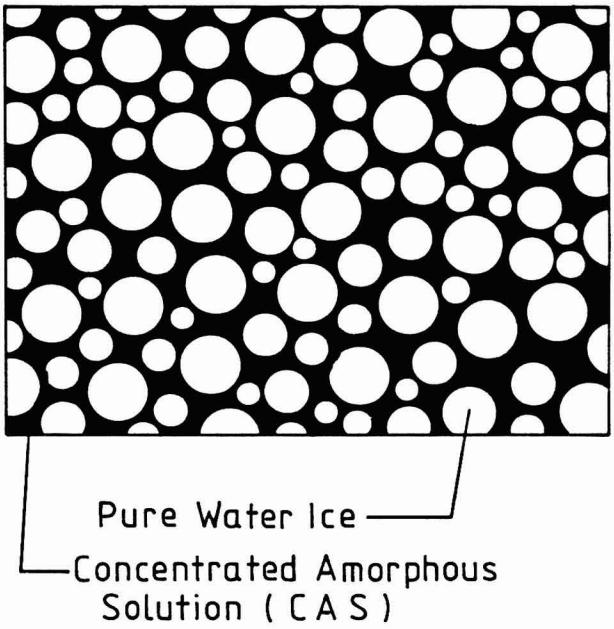

FIG. 4. A DISPERSE SYSTEM OF ORANGE JUICE ICE
Pure water ice particles are dispersed in CAS matrix.

by a factor of 15 or more. In contrast, E_{CAS} is smaller than E_{pw} by a factor of 50 or more at temperatures above $-40°C$. From $-150°C$ to $-40°C$, E_{CAS} shows a sharp decrease. The value of elastic modulus of deeply cooled CAS is comparable to that of selected metals such as palladium (121×10^9 N/m^2), gold (80×10^9 N/m^2), and aluminum (69×10^9 N/m^2) (Gray 1972).

A stress pulse propagation model for cryo-comminution of orange juice ice has been examined (Watanabe and Sakai 1991) using the elastic moduli data shown in Fig. 5.

REFERENCES

BELLOWS, R. J. and KING, C. J. 1972. Freeze-drying of aqueous solutions. Cryobiology, *9*, 559–561.

CHEN, C. S. 1985. Thermodynamic analysis of the freezing and thawing of foods: Ice content and Mollier diagram. J. Food Sci. *50*, 1163–1166.

DIBENEDETTO, A. T. 1967. *The Structure and Properties of Materials*. p. 295, McGraw Hill, New York.

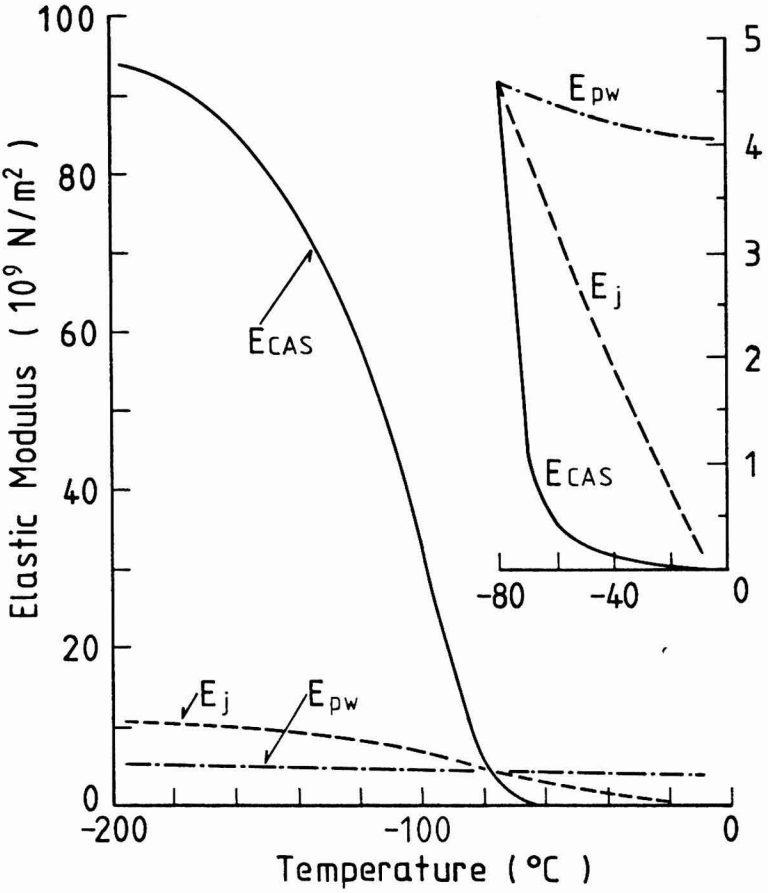

FIG. 5. ELASTIC MODULUS OF CAS AT TEMPERATURES BETWEEN −196°C AND −10°C

GOLD, L. W. 1977. Engineering properties of fresh-water ice. J. Glaciology. *19*, 197–212.

GRAY, D. E. (ed.) 1972. *American Institute of Physics Handbook*. 3rd ed. pp. 2–76, McGraw Hill, New York.

HAGIHARA, N. 1982. Development of foodstuffs by use of cryo-grinding system. Nyu Fudo Indasutori. *24*, 24–28.

HANSEN, T. C. 1965. *Proceedings of the International Conference on Structure of Concrete*, p. 16. Imperial College, London.

LONSDALE, K. 1958. Structure of ice. Proc. Roy. Soc. *247A*, 424–434.

SYNOWIETZ, C. 1977. Densities of binary aqueous systems. In *Landort-Boernstein. Numerical Data and Functional Relationships in Science and Technol-*

ogy. New series, IV/1b, (K. Schafer, ed.) pp. 202–203, Springer-Verlag, Berlin.

WATANABE, H., HAGURA, Y., ISHIKAWA, M. and SAKAI, Y. 1987. Cryogenic separation of citrus fruit into individual juice sacs. J. Food Proc. Eng. *9*, 221–229.

WATANABE, H. and SAKAI, Y. 1991. A one-dimensional stress pulse propagation model for cryo-comminution of agglomerated granules into individual granules. J. Food Proc. Eng. *14*, 9–19.

A ONE-DIMENSIONAL STRESS PULSE PROPAGATION MODEL FOR CRYO-COMMINUTION OF AGGLOMERATED GRANULES INTO INDIVIDUAL GRANULES

HISAHIKO WATANABE[1] and YOSHIO SAKAI

Department of Food Science and Technology
Tokyo University of Fisheries
4-5-7, Konan, Minato, Tokyo, 108 Japan

Accepted for Publication February 1, 1991

ABSTRACT

An elementary theory of stress pulse propagation was applied to a one-dimensional mathematical model for cryo-comminution of agglomerated granules into individual granules. An assembly of granules is approximated by a bar constructed with blocks stuck together. When an impulsive loading is given at one end of the bar, a compressive stress pulse generates there and propagates through the bar. When it survives after transmitting through the interfaces between blocks and reaches the opposite free end, the compressive stress pulse turns into a tensile stress. This tensile stress causes separation of the block located farthest away from the loading end, provided the intensity of the stress pulse exceeds the tensile strength of the material. The model successfully explained the experiment on shattering orange juice ice as well as frozen citrus fruit.

INTRODUCTION

Most applications of cryo-comminution in the food industry are the grinding of foodstuffs into their fine powders for maintaining their good quality (Hagihara 1982). Another application of cryo-comminution is the separation of agglomerated granules into individual units. In Japan, separated intact juice sacs of citrus fruits obtained through cryo-comminution are used commercially as a special ingredient for citrus fruit beverages.

Watanabe *et al.* (1987) studied the effect of temperature on cryo-comminution of citrus fruit into individual juice sacs. They found that: (a) most fragments obtained by shattering frozen citrus fruit consisted of individual intact juice sacs,

[1]Correspondence should be sent to: Hisahiko Watanabe, Dept. Food Sci. & Technol, Tokyo Univ. of Fisheries, 4-5-7, Konan, Minato, Tokyo, 108 Japan.

Journal of Food Process Engineering **14** (1991) 9–19. *All Rights Reserved.*

(b) separation occurred only below a threshold temperature (−40°C), and (c) the shattering of citrus juice ice cubes took place at a temperature below a similar threshold (−35°C) as that of citrus fruit shattering. Recently, Watanabe *et al.* (1991) measured elastic modulus of orange juice ice. They determined elastic modulus of concentrated amorphous solution (CAS) (Bellows and King 1972) assuming that orange juice ice consisted of pure water ice particles dispersed in CAS matrix.

In the present paper, an elementary theory of stress pulse propagation was applied to a one-dimensional mathematical model for comminution of agglomerated granules. The application of the model to shattering orange juice ice cubes was examined by use of the data reported by Watanabe *et al* (1991).

DESCRIPTION OF THE MODEL

For the present analysis, an assembly of juice sacs was approximated by blocks stuck together (Fig. 1).

Propagation of a Stress Pulse Through an Elastic Bar

When an impulsive loading is given at an end of the bar constructed by fixing one end of block 1 to an end of block 2 (Fig. 2A), a compressive stress generates there. The stress is given by Eq. (1) according to Kolsky (1963):

$$\sigma_o = (\rho E)^{1/2} u_o \tag{1}$$

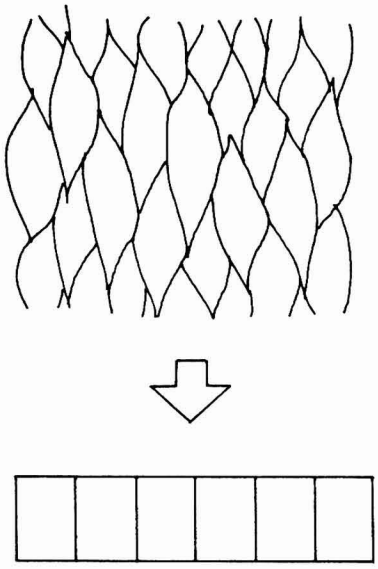

FIG. 1. AN ASSEMBLY OF CITRUS JUICE SACS APPROXIMATED BY BLOCKS STUCK TOGETHER

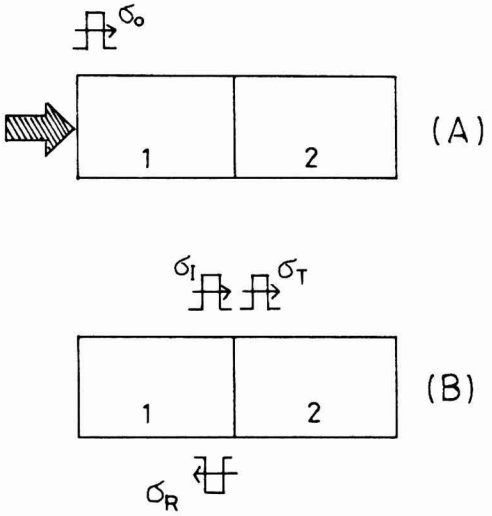

FIG. 2. AN IMPULSIVE LOADING GIVEN AT AN END OF A BAR CONSTRUCTED BY FIXING TWO BLOCKS 1 AND 2 (A)
Transmission and reflection of a stress pulse at an interface between 1 and 2 (B).

where E is elastic modulus, ρ is density of the block and u_o is the velocity of element displacement at the loading end.

The generated stress pulse travels through the block 1 and when it reaches the interface between the two blocks, 1 and 2, transmission and reflection of the pulse take place there (Fig. 2B). The transmitted stress pulse, σ_T, and reflected stress pulse, σ_R, are related to incident stress pulse, σ_I, by Eq. (2) and (3) (Nakahara 1977):

$$\sigma_T = \frac{2(\rho_2 E_2)^{1/2}}{(\rho_1 E_1)^{1/2} + (\rho_2 E_2)^{1/2}}\sigma_I \tag{2}$$

$$\sigma_R = \frac{2(\rho_2 E_2)^{1/2} - (\rho_1 E_1)^{1/2}}{(\rho_1 E_1)^{1/2} + (\rho_2 E_2)^{1/2}}\sigma_I \tag{3}$$

where the subscripts 1 and 2 denote the first and second blocks.

Reflection at a Free End

When a compressive stress pulse reaches a free end, as in the case where the block 2 is air, Eq. (2) and (3) become:

$$\sigma_T = 0 \tag{4}$$

$$\sigma_R = -\sigma_I \tag{5}$$

because $\rho_2 E_2$ is nearly zero. The reversal of sign of the stress pulse means that the compressive stress changed into a tensile stress (Fig. 3).

Separation of Blocks due to Fracture

Tensile stress rather than compressive stress causes the fracture because materials are usually much weaker in tensile strength than in compressive strength (Richards 1961a).

The tensile stress pulse, which is generated at the free end of the block n by reflection (Fig. 4), travels through the block in the reverse direction. When it reaches a place where the stress pulse exceeds the tensile strength, separation of a fragment from the bar takes place due to the fracture there. The separated fragment includes the block n located at the free end (Fig. 4).

APPLICATION OF THE MODEL TO SHATTERING ORANGE JUICE ICE

Orange juice ice could be considered to consist of pure water ice particles which are dispersed in CAS matrix (Fig. 5A). A one-dimensional model for orange juice ice is given by a bar made up of blocks A (pure water ice) and B (CAS) each of which sticks one by one (Fig. 5B).

Decay of Stress Pulse Propagating Through the Interfaces Between Blocks of Pure Water Ice and CAS

When the compressive stress pulse, σ_{oA}, generated at the loading end, i.e., the left-hand side end of the bar, passes the interface between A and B after it travels through A, the transmitted stress, σ_{oB}, is given by Eq. (6) according to Eq. (2):

$$\sigma_{oB} = \frac{2(\rho_B E_B)^{1/2}}{(\rho_A E_A)^{1/2} + (\rho_B E_B)^{1/2}} \cdot \sigma_{oA} \tag{6}$$

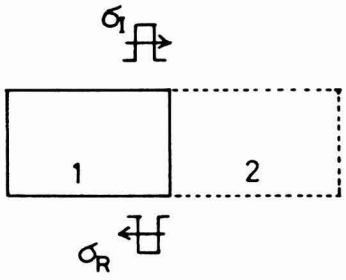

FIG. 3. REFLECTION OF STRESS PULSE AT A FREE END

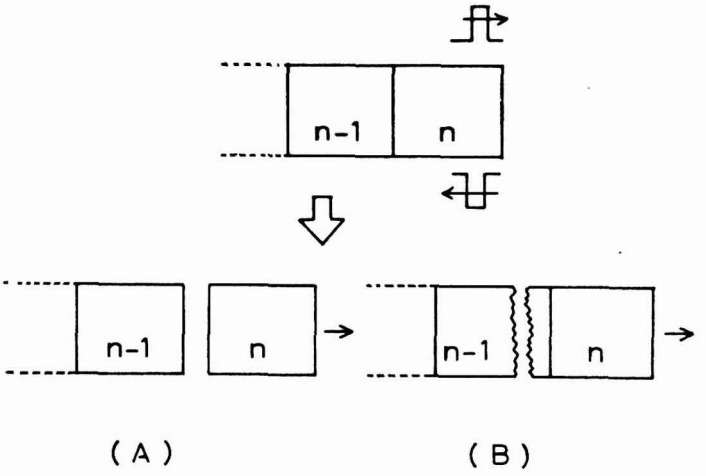

FIG. 4. SEPARATION OF THE BLOCK n DUE TO FRACTURE AT A JOINT (A), OR AT SOMEWHERE IN THE BLOCK n-1 (B)

This reaches the interface between B and the second block A after travelling through B. The stress transmitted through this interface, σ_{1A}, is given by Eq. (7) in the same way as above.

$$\sigma_{1A} = \frac{2\,(\rho_A E_A)^{1/2}}{(\rho_A E_A)^{1/2} + (\rho_B E_B)^{1/2}} \cdot \sigma_{oB} \tag{7}$$

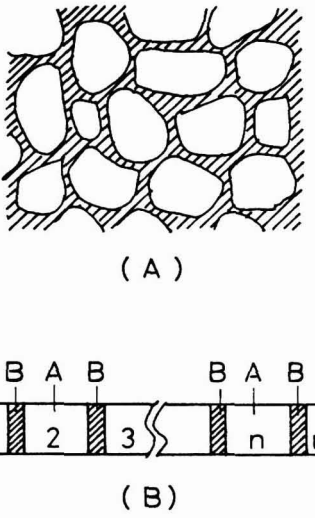

FIG. 5. ORANGE JUICE ICE WHICH CONSISTS OF PURE WATER ICE PARTICLES DISPERSED IN CAS MATRIX (A)
A bar made up of blocks A (pure water ice) and B (CAS) as a one-dimensional model of orange juice ice (B).

After the stress pulse passes through a couple of interfaces between A and B and between B and A, its intensity decreases by a factor of φ_1:

$$\varphi_1 = \frac{\sigma_{1A}}{\sigma_{oA}} = \frac{4\,(\rho_B E_B \rho_A^{-1} E_A^{-1})^{1/2}}{(1 + (\rho_B E_B \rho_A^{-1} E_A^{-1})^{1/2})^2} \tag{8}$$

After transmitting n couples of interfaces, the stress pulse decays by a factor of φ_n:

$$\varphi_n = \frac{\sigma_{nA}}{\sigma_{oA}} = (\varphi_1)^n \tag{9}$$

From Eq. (1), (8), and (9), we obtain the stress pulse transmitted through n couples of interfaces, σ_n:

$$\sigma_n = u_o(\rho_A E_A)^{1/2}[4(\rho_B E_B \rho_A^{-1} E_A^{-1})^{1/2}(1 + \rho_B E_B \rho_A^{-1} E_A^{-1})^{-2}]^n \tag{10}$$

Equation (10) describes the stress pulse which survives after it travels through orange juice ice consisting of n blocks of B and n + 1 blocks of A as in Fig. 5B.

Threshold Temperature for Shattering Orange Juice Ice

Richards (1961a) has described that brittle materials are stronger in compression than in tension sometimes by a large factor, namely, compressive strength is much larger than tensile strength. In addition, it has been shown that tensile strength has a value which is approximately one thousandth of elastic modulus as listed in Table 1 (Richards 1961b).

Suppose the left side end of a bar of orange juice ice, which is cooled to a temperature ranging from -10°C to -80°C, is struck by a ball with a velocity

TABLE 1.
ELASTIC MODULUS AND TENSILE STRENGTH
OF SELECTED MATERIALS (Richards 1961b)

Material	Elastic modulus	Tensile strength	
	$E(10^6$ psi)	$\sigma_t(10^3$ psi)	$\frac{\sigma_t}{E/10^3}$
Alumina ceramics	45	40	0.9
Molded graphite	0.8	0.6	0.75
Polycrystalline glass	12,5	20	1.6
Steel	30	70	2.3

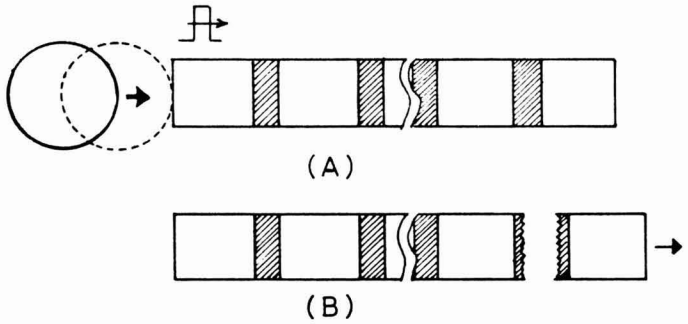

FIG. 6. A COMPRESSIVE STRESS PULSE GENERATED BY A BLOW ON AN END OF A BAR (A)
Separation of pure water ice block from the bar due to the fracture in a CAS block (B).

u_o (Fig. 6A). The impact generates a compressive stress pulse, σ_o. If σ_o is smaller than compressive strength of CAS, which is smaller than that of pure water ice at a temperature above $-80°C$ (Watanabe *et al.* 1989), the stress pulse travels through the bar but does not fracture it. When the stress pulse reaches the opposite free end after traveling n couples of interfaces between pure water ice blocks and CAS blocks, it turns into tensile stress, σ_n, which is given by Eq. (10). The tensile stress travels back and meets the CAS block located farthest from the loading end. When σ_n is larger than the tensile strength of CAS, the CAS block fails by fracture even though the tensile stress is well below its compressive strength. The pure water ice block separates from the assembly (Fig. 6B).

When many stress pulses are generated successively at the rough surface of the loading end (Fig. 7A), these pulses break the CAS blocks one after another (Fig. 7B).

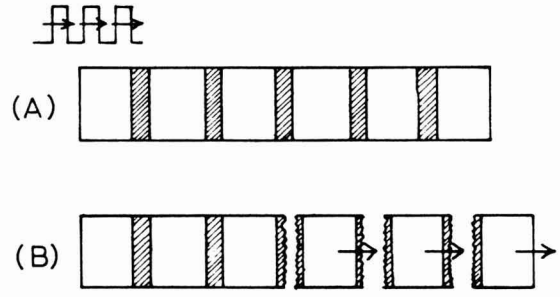

FIG. 7. MANY STRESS PULSES GENERATED SUCCESSIVELY AT THE LOADING END (A)
Separation of pure water ice blocks one by one (B).

The values of σ_n at various temperatures were determined by Eq. (10). A velocity which is equivalent to that of a ball falling one meter (Watanabe *et al.* 1987) was used as u_o. Density of pure water ice, ρ_A, and CAS, ρ_B, were estimated by the method described elsewhere (Watanabe *et al.* 1991). Elastic modulus of pure water ice, E_A, and CAS, E_B, measured by Watanabe *et al.* (1991) were used.

The calculated values of σ_n are plotted against temperature in Fig. 8 for n from 0 to 16. Figure 8 shows the effect of temperature as well as of the number of couples of interfaces on the stress pulse at the free end. Estimated values for tensile strength of CAS, σ_{CAS}*, as well as selected σ_n are plotted in Fig. 9. The tensile strength σ_{CAS}* was estimated by:

$$\sigma_{CAS}^* = E_{CAS}/10^3 \tag{11}$$

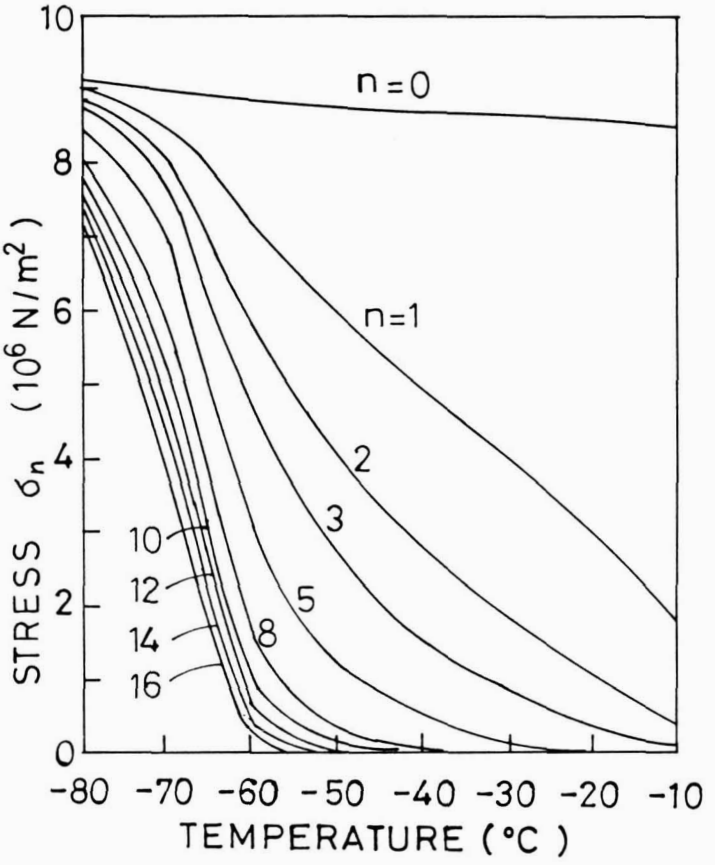

FIG. 8. STRESS PULSE AT THE FREE END AFTER PROPAGATING THROUGH n COUPLES OF INTERFACES BETWEEN PURE WATER ICE AND CAS

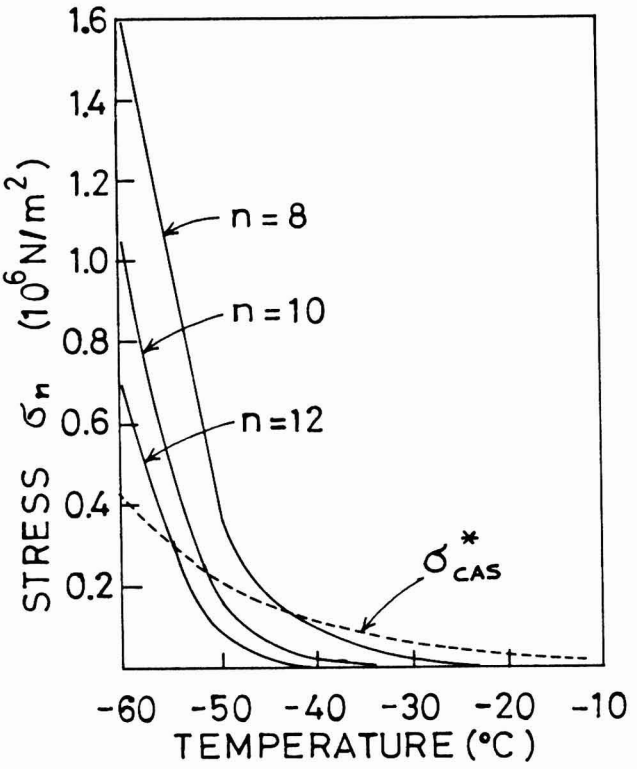

FIG. 9. ESTIMATED VALUES FOR TENSILE STRENGTH OF CAS DETERMINED BY EQ. (11) AND FOR SELECTED STRESS PULSES AT THE FREE END

The intercepts of the curves for σ_n and for σ_{CAS}* give the threshold values for shattering.

Figure 9 indicates that the predicted threshold temperature for shattering is -45°C if n is eight and -52°C if n is ten. Considering that the σ_{CAS}* curve is estimated in round figures, the predicted threshold temperature successfully agrees with the experimental result (Watanabe *et al.* 1987), provided that the number of couples of interfaces n is around ten.

The height of orange juice cubes divided by the number of couples of interfaces n gives the size of pure water ice particle in orange juice ice, because pure water ice is dominant in volume fraction. Since the orange juice cube used in the experiment (Watanabe *et al.* 1987) was 20 mm in height, the size of pure water ice particles is estimated around 2 mm when n is around ten. This agrees favoraby with the experimental observation: in the shattering orange juice ice experiment, fragments smaller than 2 mm were discarded because they were too small to be regarded as agglomerating units (Watanabe *et al.* 1987).

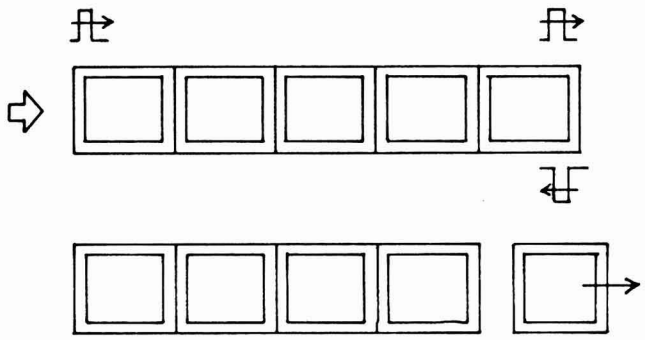

FIG. 10. A ONE-DIMENSIONAL MODEL OF FROZEN CITRUS FRUIT JUICE SACS
A stress pulse generated at the loading end propagates through the blocks and causes separation of the block located farthest from the loading end.

APPLICATION OF THE MODEL TO SHATTERING CITRUS FRUIT INTO JUICE SACS

Watanabe *et al.* (1987) reported that most fragments obtained by shattering frozen citrus fruit consisted of separate intact juice sacs. This fact is explained successfully when the model is applied to shattering frozen citrus fruit.

Figure 10 represents a one-dimensional model of frozen citrus fruit juice sacs which consist of juice sac membranes and blocks of juice ice covered by them. A compressive stress pulse generated at the left end propagates through blocks of frozen juice sacs. When the stress pulse survives after the propagation to the opposite free end, it turns there into a tensile stress. If the tensile stress is larger than the strength of joints between sacs, it causes separation of the block located farthest from the impact end in the same manner as described above. Because the separation takes place one by one at the outer most block, the separated fragments consist of individual juice sacs.

Concerning the threshold temperature for shattering citrus fruit juice sacs, however, we have no means of ascertaining it because the elastic modulus of orange juice sac membrane and tensile strength of joints between juice sacs are not available.

ACKNOWLEDGMENT

The authors express their deep thanks to Professor Hiroshi Fukuda, Science University of Tokyo, and Dr. S. C. Spaeth, Grain Legume Genetics and Physiology Research, ARS, for their invaluable discussions.

REFERENCES

BELLOWS, J. R. and KING, C. J. 1972. Freeze drying of aqueous solution: Maximum allowable operating temperature. Cryobiology, *9*, 559–561.

CHEN, C. S. 1985. Thermodynamic analysis of the freezing and thawing of foods: Ice content and Mollier diagram. J. Food Sci. *50*, 1163–1166.

HAGIHARA, N. 1982. Development of foodstuffs by use of cryogenic grinding system, Nyu Fudo Indasutori, *24* (11), 24–28.

KOLSKY, H. 1963. *Stress Waves in Solids*. pp. 41–46, Dover Publications, New York.

NAKAHARA, I. 1977. *Oyo Danseigaku*. pp. 190–197, Jikkyo Shuppan, Tokyo.

RICHARDS, C. W. 1961a. *Engineering Material Science*. p. 151, Wadsworth Publishing Co., San Francisco.

RICHARDS, C. W. 1961b. *Engineering Material Science*. p. 520, Wadsworth Publishing Co., San Francisco.

WATANABE, H., HAGURA, Y., ISHIKAWA, M., MIHORI, T. and SAKAI, Y. 1991. Elastic modulus of orange juice ice. J. Food Proc. Eng. *14*, 1–8.

WATANABE, H., HAGURA, Y., ISHIKAWA, M. and SAKAI, Y. 1987. Cryogenic separation of citrus fruit into individual juice sacs. J. Food Proc. Eng., *9*, 221–229.

EFFECT OF pH AND ENZYMATIC TREATMENT ON MICROFILTRATION AND ULTRAFILTRATION OF TANGERINE JUICE

M. CHAMCHONG and DR. ATHAPOL NOOMHORM

Division of Agricultural and Food Engineering
Asian Institute of Technology
G.P.O. Box 2754, Bangkok
Thailand 10501

Accepted for Publication February 1, 1991

ABSTRACT

*Tangerine (*Citrus reticulata *blanco) juice clarification by crossflow microfiltration and ultrafiltration using polysulphone flat sheet membranes with nominal molecular weight cut off of 25,000, 50,000, 100,000 and 0.1 μm, 0.2 μm pore sizes was studied. The juice was pretreated by polygalacturonase and pH adjustment. The treated juice was clarified with a laboratory scale filtration unit with effective filtration area of 14 cm^2. Filtration conditions were transmembrane pressure of 93 to 194 kPa, crossflow velocity of 0.96 to 3.5 m/s and 25°C. Membrane performance was evaluated in terms of volume flux and clarity (% transmittance) of the permeate.*

Pretreatment of the juice by polygalacturonase and adjustment to pH 2 with HCl resulted in a clearer supernatant than enzyme treatment alone. Maximum flux was obtained with the 0.1 μm microfiltration membrane. Flux increased with transmembrane pressure and crossflow velocity. Flux at 194 kPa and 3.5 m/s was 69 L per square meter per hour. Permeate clarity was better at higher transmembrane pressure and lower velocity, due to the effect of the polarized/fouling layer of solute on the membrane surface, which acted as a secondary "dynamic" filter.

INTRODUCTION

Tangerine juice is of commercial and nutritional importance in the tropics, due to its excellent taste and as a natural source of vitamin C and other important nutrients. Processing and handling of the juice could affect the quality of the product as shown by several studies on the preservation of the juice nutrients,

Journal of Food Process Engineering **14** (1991) 21–34.

color, texture and flavor as well as with packaging, storage and transportation (Lund 1977). Reduction of product volume using conventional methods such as evaporation results in losses of many desirable compounds due to thermal exposure and development of undesirable compounds such as furfurals (Beveridge and Harrison 1986). These limitations can be avoided by using freeze drying and membrane concentration.

Application of microfiltration and ultrafiltration as pretreatments for pulp removal, and subsequent concentration of orange juice serum by reverse osmosis has gained wide interest, as the process results in a high quality product and is energy efficient. Recent studies in filtration of fruit juices for pretreatment and concentration processes involves the use of ultrafiltration and reverse osmosis (Medina and Garcia 1988). No appreciable color, aroma and flavor loss was observed during the process as the system does not involve phase change nor heat application (Kirk *et al.* 1983). However, only part of the oil soluble flavor compounds are retained by UF membrane, possibly due to their association with the macromolecules (Yu *et al.* 1986). A two stage concentration process involving ultrafiltration (UF) with reverse osmosis (RO) was suggested as the best system.

The advantages of crossflow UF of fruit juice include low operating cost, low labor requirements and excellent retention of fresh product quality and appearance (Rao *et al.* 1987). Feed pretreatment either by chemical reaction, centrifugation or pre-filtration is very important to minimize fouling of the membrane. This paper reports on a study of the effect of different parameters on the performance of crossflow ultrafiltration in clarification of tangerine juice. A laboratory scale system was used. The results will be useful in obtaining scale-up information, on the use of membrane filtration for clarification of tangerine juice.

MATERIALS AND METHODS

Tangerine Juice Samples for Clarification

Approximately 200 L of tangerine juice was taken from the commercial processing line before pasteurization and kept in storage conditions of $-10°C$. Samples for clarification studies were thawed and passed through a sieve (mesh = 0.5mm) to remove physical impurities such as seeds, rag and pulp. Samples were added with 0.02% sodium benzoate to control microorganism growth.

Filtration Unit

The laboratory scale filtration system is shown in Fig. 1. The system involves a rectangular membrane unit made from acrylic resin, with effective area of 14 cm^2. Polysulfone membranes (DDS Filtration, Denmark) with nominal molecular

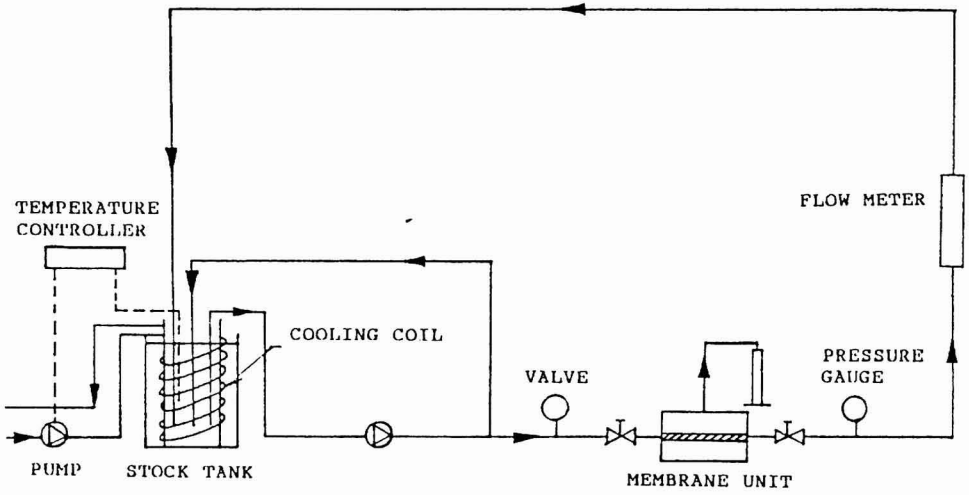

FIG. 1. SCHEMATIC DIAGRAM OF EXPERIMENTAL SET-UP

weight cut off or pore size of 25,000, 50,000, 100,000 and 0.1 μm, 0.2 μm were used. A centrifugal pump of 29 L/min. maximum capacity and 227 kPa maximum pressure was attached to the unit.

Filtration System

Tangerine juice from the stainless steel stock tank was pumped into the crossflow ultrafiltration unit. The permeate was collected and the rest of the sample was recycled back to the stock tank. The system was operated under controlled temperature conditions of $25 \pm 1°C$ using a thermo-controlled water bath and cooling system.

Sample pretreatment was done with half of the tangerine juice samples acidified with hydrochloric acid (HCl) to pH of 2 and kept standing for 30 min to stabilize. The pH was subsequently raised to 4 to provide the best condition for enzyme activation (Pectinex™ Ultra SP-L, Novo, Switzerland). Part of the pH adjusted sample was treated with this enzyme, and the rate of enzyme reaction, its concentration and activation time were determined by comparing the cloud loss with respect to nonenzyme treated sample (control) using a spectophotometer (Model PU8600, Pye Unicam LTD, England). The enzyme treated juice had to be prefiltered or clarified by using crossflow microfiltration or ultrafiltration. However, since the filtration unit was not suitable for acid solutions, the pH of treated juice was adjusted to 7 before membrane filtration. The filtrate for each run was taken and tested for its clarity. The experimental design for this study is shown in Fig. 2.

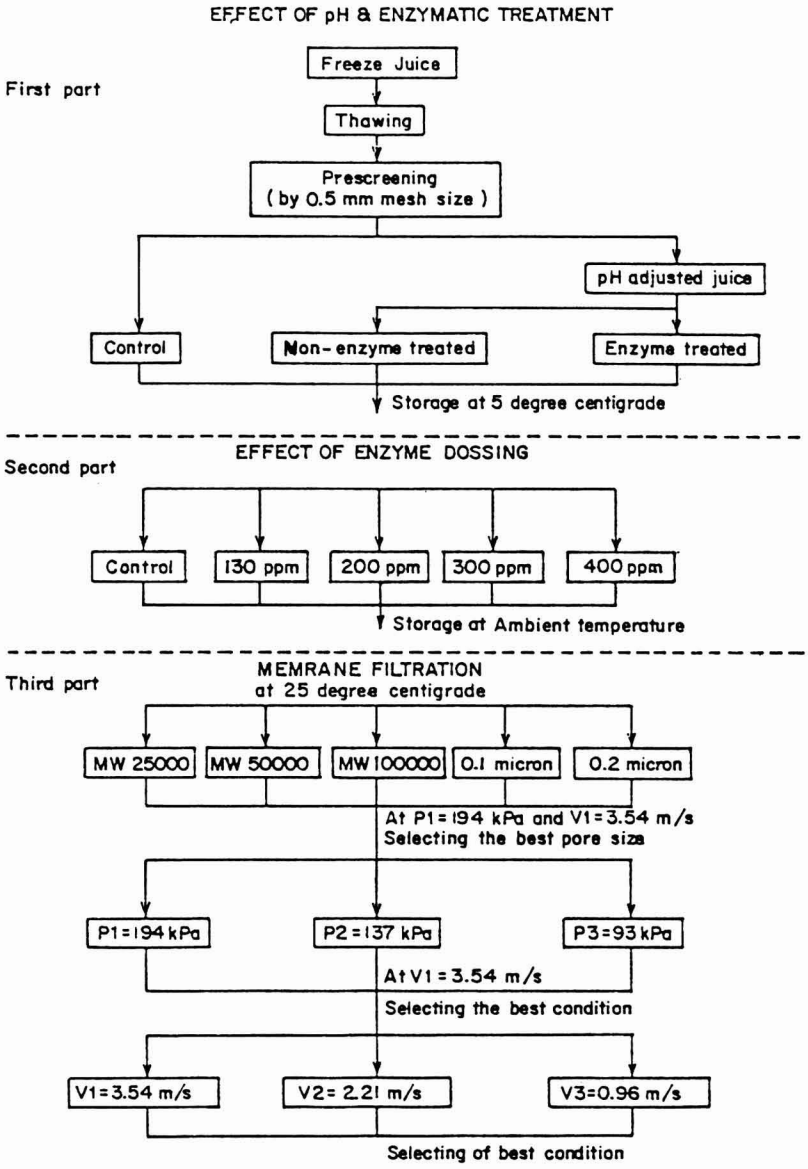

FIG. 2. EXPERIMENTAL DESIGN FOR TANGERINE JUICE CLARIFICATION

Quality Evaluation of Tangerine Juice Supernatant and Permeate

Single strength tangerine juice samples (13° Brix) were obtained to determine its initial chemical and physical characteristics in term of pH, % suspended solids, % total dissolve solids, viscosity and density.

Supernatant obtained from centrifugation of the fresh tangerine juice were used on cloud loss determination. Approximately 10 mL portion of treated single strength juice was centrifuged at a speed of 4,000 rpm for 10 min. The supernatant was then filtered through Whatman No. 41 filter paper (Whatman Limited, England). The cloud loss was measured from the filtrate by determining % transmittance at 660 nm wavelength on a spectophotometer with distilled water as blank (Versteeg *et al.* 1980 as cited by Owusu *et al.* 1988).

Permeate from membrane filtration unit was measured for flux, and clarity. Clarity measurement was done with the same procedure as with cloud loss but without the use of filter paper.

RESULTS AND DISCUSSION

Enzyme Treatment

Cloud loss profiles for each treatment measured as % transmittance is shown in Fig. 3. Tangerine juice with pH and enzyme treatment gave the highest average transmittance of 92.6%, compared to 76.3% for the enzyme treated juice and 43.8% for the control. Cloudiness is affected by both pH and enzyme (exogenous and endogenous). At low pH, enzymes can depolymerize and break up the pectin and cellulose (Doesburg 1965; Bruemmer *et al* 1976; Bella *et al.* 1980).

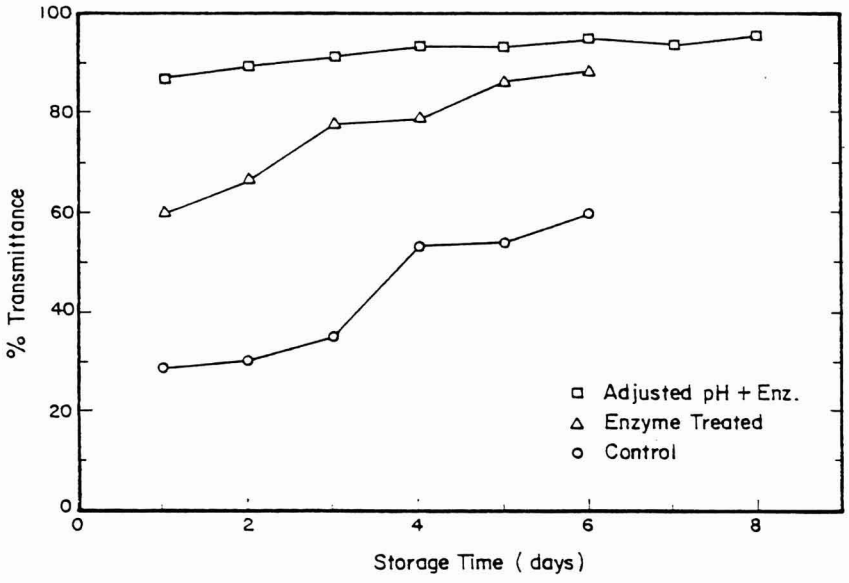

FIG. 3. EFFECT OF pH ADJUSTMENT AND ENZYMATIC TREATMENT ON CLOUD LOSS

The effect of enzyme concentration is shown in Fig. 4. The clarity (% transmittance) for all treatments showed a relatively constant value of 87–90% after 3 h. Based on the cost and end point of reaction an enzyme concentration of 130 ppm and reaction time of 3 h was selected.

Effect of Membrane Pore Size

Initial experiments were conducted to select the best pore size based on flux and permeate clarity. With all membranes, there was an initial rapid drop in flux in the first 60 min, followed by relatively steady flux (typical fouling pattern is shown later in Fig. 7). Figure 5 shows the steady-state flux for each membrane. Particles of 1 μm and above were observed in the pH-enzyme treated juice, which could have plugged the pores of the 0.2 μm membrane, accounting for its lower flux. Permeate quality (% transmittance) improved with filtration time for all membranes (Fig. 6). Eventually, it was observed that all membrane filters gave approximately the same permeate quality. Based on these results, it was decided to use the 0.1 μm microfiltration membrane for further study, since it gave the best combination of flux and permeate quality.

Effect of Transmembrane Pressure

The flux obtained at various transmembrane pressures is shown in Fig. 7. The average steady flux at transmembrane pressure of 93, 137, and 194 kPa was 48,

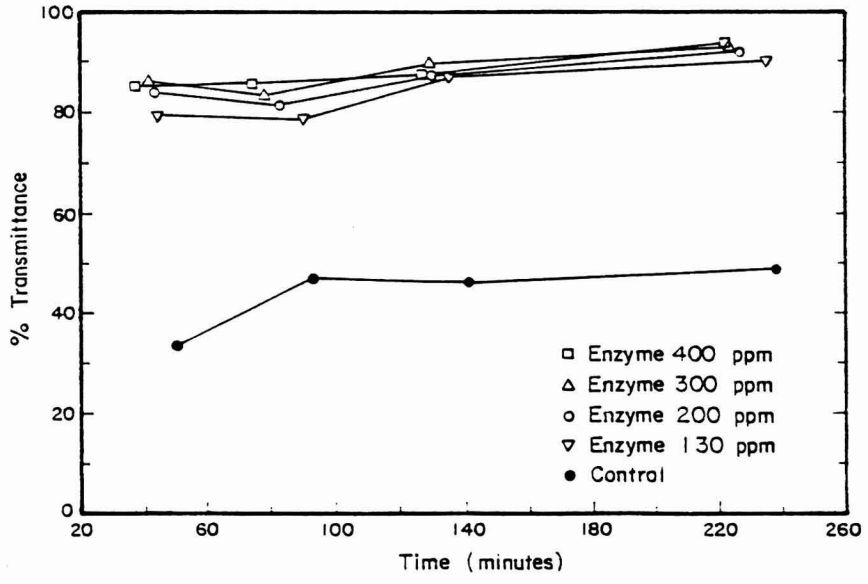

FIG. 4. ACTIVATION TEST OF ENZYME DOSING

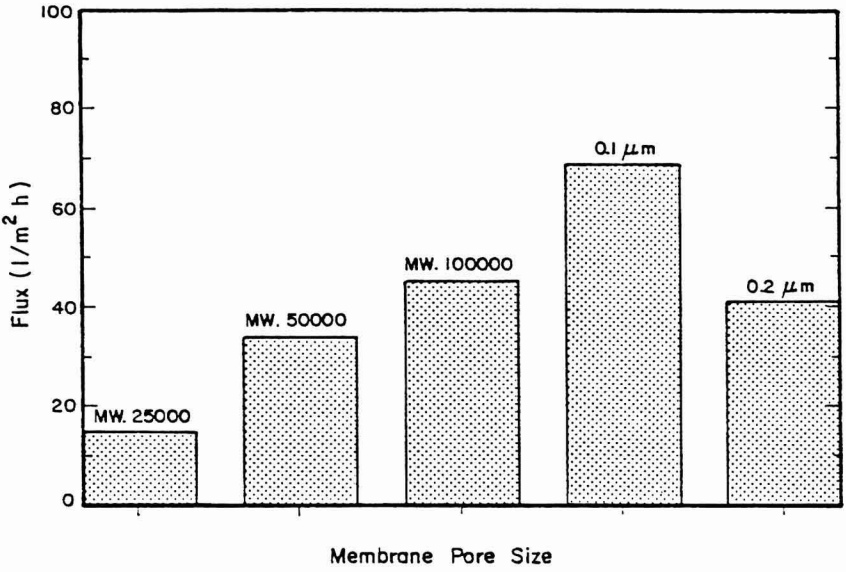

FIG. 5. EFFECT OF PORE SIZE ON FLUX (AT TRANSMEMBRANE PRESSURE OF 194 kPa, CROSSFLOW VELOCITY OF 3.5 m/s AND 25°C)

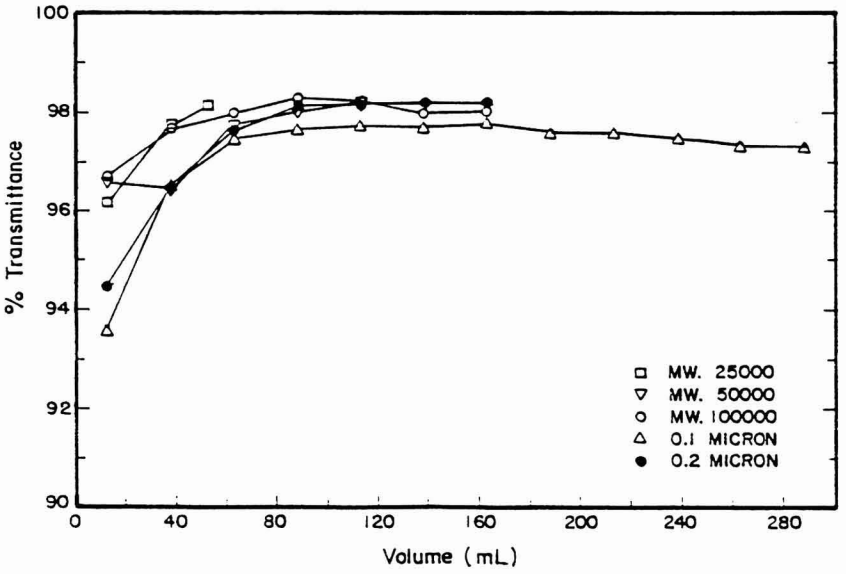

FIG. 6. EFFECT OF PORE SIZE ON % TRANSMITTANCE (AT TRANSMEMBRANE PRESSURE OF 194 kPa, CROSSFLOW VELOCITY OF 3.5 m/s AND 25°C)

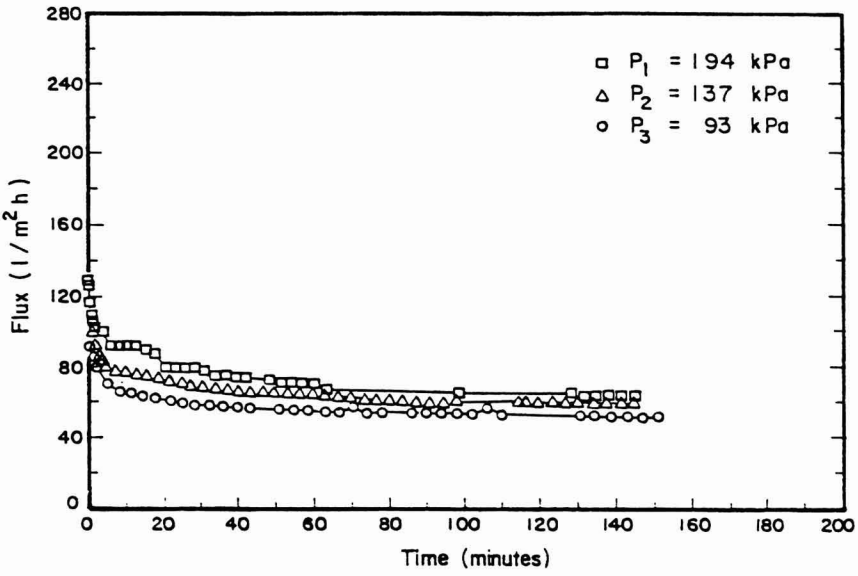

FIG. 7. EFFECT OF TRANSMEMBRANE PRESSURE ON FLUX (AT 0.1 μm MEMBRANE PORE SIZE, CROSSFLOW VELOCITY OF 3.5 m/s and 25°C)

59 and 66 1 $m^{-2}h^{-1}$, respectively. Theoretically, a further increase in the transmembrane pressure should result in higher flux. However, after a critical level of transmembrane pressure the permeate flux will be independent of the pressure, due to concentration polarization of macromolecules on the membrane surface (Cheryan 1986). Jenson and Bossen (1984) and Lee and Atkinson (1985) had stated that it is likely that UF flux may be limited by the osmotic pressure in addition to the formation of a gel layer, depending on the nature of the solute and operating conditions.

The permeate quality (transmittance) during the initial stages (first 90 mL of cumulative volume) to steady stage, is shown in Fig. 8. An improvement (≈4% transmittance) in permeate quality in the initial stage for each level of transmembrane pressure was observed. However, after 60 min, clarity of flux in steady stage was affected by transmembrane pressure and other factors, i.e., concentration polarization and gel formation. However, lower transmembrane pressure of 134 kPa could produce the same permeate quality but less quantity when compared with 194 kPa. The selection of transmembrane pressure will therefore depend on the requirements of the system and limitations of time and cost.

Effect of Crossflow Velocity

Figure 9 shows the effect of crossflow velocity on flux. The highest velocity (3.5 m/s) resulted in the highest flux. After 2.5 h filtration time, flux was 72 l/

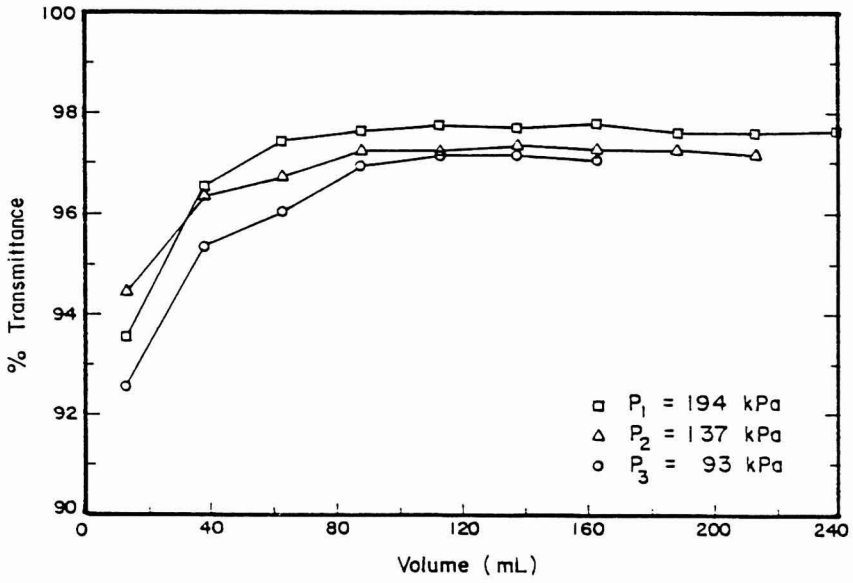

FIG. 8. EFFECT OF TRANSMEMBRANE PRESSURE ON % TRANSMITTANCE (AT 0.1 μm MEMBRANE PORE SIZE, 3.5 m/s MEMBRANE CROSSFLOW VELOCITY AND 25°C)

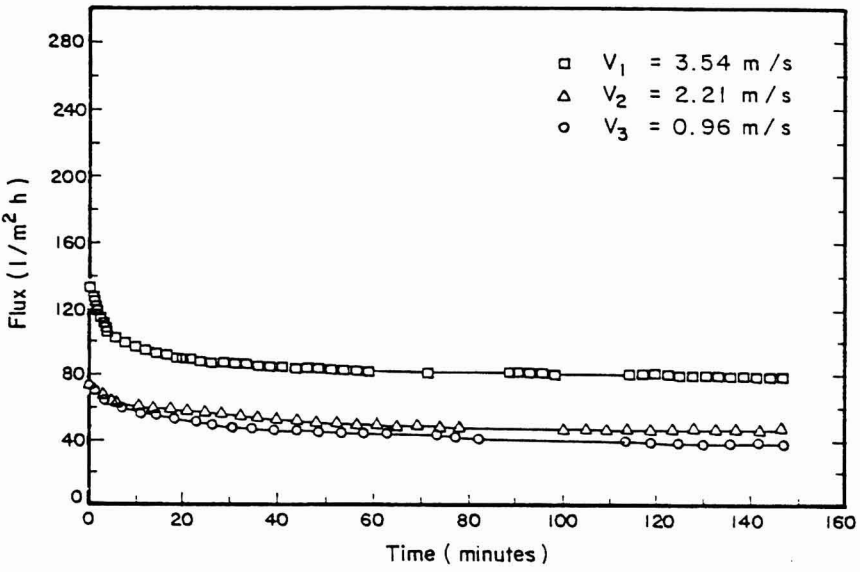

FIG. 9. EFFECT OF CROSSFLOW VELOCITY ON FLUX (AT TRANSMEMBRANE PRESSURE OF 194 kPa, 0.1 μm MEMBRANE PORE SIZE AND 25°C)

m^2h at 3.5 m/s crossflow velocity, 46 l/m^2 at 2.2 m/s and 35 l/m^2h at 0.9 m/s. Higher crossflow velocity retards fouling layer formation on membrane surface.

During initial stage of filtration (first 60 mL volume of filtrate), crossflow velocity of 3.5 m/s had the most improvement in the transmittance (≈13%), then followed by 2.2 and 0.9 m/s, as shown in Fig. 10. Improvement in transmittance for 2.2 and 0.9 m/s were not significantly different (≈4%), thus it can be concluded that at low crossflow velocity, the occurrence of boundary and gel layer have more effect on the clarity than at high crossflow velocity conditions.

Membrane Resistance and Hydraulic Resistance of Particle Layer

The movement of solute through membranes is affected mainly by solute and membrane characteristics. Analysis of the quantity of movement is also affected by operating parameters. Generally, membrane resistance (R_m) and hydraulic resistance of particle layer (R_L) are the major resistances to flow of permeate.

Flux in crossflow microfiltration can be modelled by Darcy's equation:

$$Jv = \frac{P_{tm}}{\mu(R_L + R_m)} \tag{1}$$

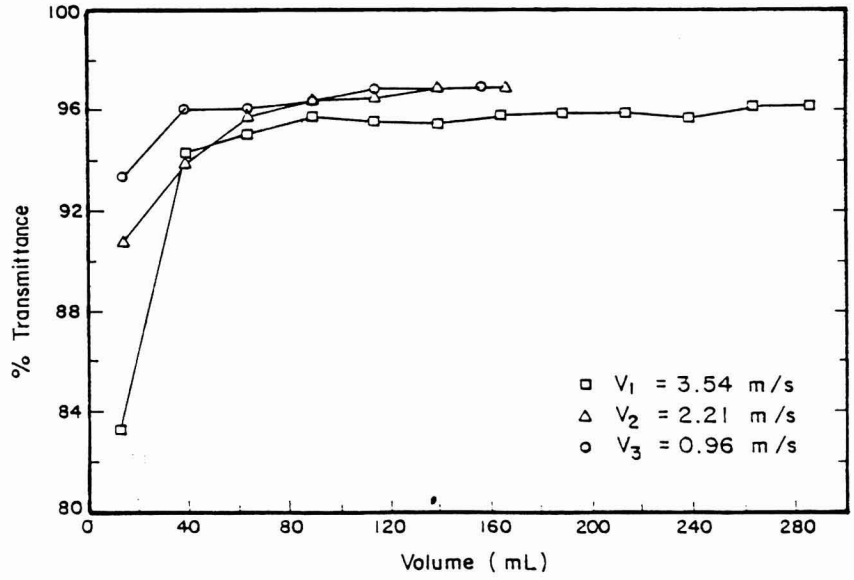

FIG. 10. EFFECT OF CROSSFLOW VELOCITY ON % TRANSMITTANCE (AT TRANSMEMBRANE PRESSURE OF 194 kPa, 0.1 μm MEMBRANE PORE SIZE AND 25°C)

It was assumed that the membrane's intrinsic properties do not change during filtration. R_m can be calculated from water flux data:

$$R_m = \frac{J_v(\text{water})}{\mu\,(P_{tm})} \tag{2}$$

Table 1 shows the membrane resistance (R_m of each membrane used in this study. Increased membrane resistance is observed with decrease in membrane pore size. As tangerine juice passed through the membrane, the permeability characteristic of membrane changed, either due to solute adsorption inside and/or on membrane or due to boundary layer and gel layer resistance. The above mentioned resistance factors can enhance hydraulic resistance of the membrane.

The effect of membrane pore size, transmembrane pressure and feed crossflow velocity on hydraulic resistance (R_L) is shown in Table 2, 3 and 4, respectively. Hydraulic resistance (R_L) for molecular weight cut off 25,000 was highest and decreased with the increase in membrane pore size up to 0.1 μm. Significant increase in R_L was also observed at 0.2 μm pore size. Therefore, filtration through 0.2 μm pore size, adsorption of solute inside and/or on membrane, the boundary and gel layer formation created more resistance to flux with respect to 0.1 μm pore size. Filtering at membrane pore size of 0.1 μm, hydraulic resistance was also affected by operating parameters i.e., transmembrane pressure and feed crossflow velocity. As P_{tm} increased, R_L was reduced, resulting to higher volume of permeate. At increased crossflow velocity, R_L was also reduced. Therefore at lowest crossflow velocity 0.9 m/s, maximum R_L of 1.755×10^{13} m^{-1} was observed. However, within the specified operating parameters in this study, R_m was relatively small compared to R_L.

TABLE 1.
MEMBRANE RESISTANCE AT EACH MEMBRANE PORE SIZE BY PURE WATER FLUX (AT CROSS FLOW VELOCITY 3.5 m/s, TEMP. 25°C)

M.W. cut-off or pore size.	Rm, Membrane Resistance (1/m)			
	P_{tm}=93 kPa	P_{tm}=137 kPa	P_{tm}=194 kPa	Avg. Rm
M.W. 25000	20.19×10^6	19.68×10^6	20.16×10^6	20.01×10^6
M.W. 50000	5.69×10^6	5.55×10^6	5.69×10^6	5.64×10^6
M.W. 100000	3.16×10^6	3.11×10^6	3.19×10^6	3.15×10^6
0.1 μm	742.40×10^3	723.73×10^3	741.38×10^3	0.74×10^6
0.2 μm	554.01×10^3	540.09×10^3	553.25×10^3	0.54×10^6

TABLE 2.
HYDRAULIC RESISTANCE (R_L) OF PARTICLE LAYER AS AFFECTED BY MEMBRANE PORE SIZE (CROSSFLOW VELOCITY 3.5 m/s, P_{tm} 194 kPa, Temp. 25°C)

M.W. cut off or pore size.	Dynamic viscosity, Cp	Flux l/m².h	$P_{tm}/J.\mu$	Hydraulic Resistance 1/m
M.W. 25000	1.144	15.01	$4.082x10^{13}$	$4.082x10^{13}$
M.W. 50000	1.190	34.06	$1.740x10^{13}$	$1.740x10^{13}$
M.W. 100000	1.195	45.26	$1.299x10^{13}$	$1.299x10^{13}$
0.1 μm	1.224	68.92	$8.423x10^{12}$	$0.842x10^{13}$
0.2 μm	1.221	41.10	$1.402x10^{13}$	$1.402x10^{13}$

CONCLUSIONS

Tangerine juice pretreatment such as pH adjustment with enzymatic treatment resulted in clearer supernatant solution after centrifugation than with enzyme treatment alone. Polygalacturonase (Pectinex™ Ultra SP-L) enzyme dosage appropriate for single strength tangerine juice was 130 ppm at pH 3.5–4 and reaction time of 3 h. Particle size of the juice was approximately 0.1–0.2 μm. Quality of permeate as measured in terms of clarity (% transmittance) was not significantly different for various membrane pore sizes. Membrane pore size of 0.1 μm which gave highest flux was used in a study of effects of other operating parameters.

As transmembrane pressure increased from 93 to 194 kPa, flux increased from 48 to 66 $L.m^{-2}h^{-1}$. Transmembrane pressure of 194 kPa gave highest transmittance of 97% but was not significantly different with 137 kPa. Furthermore, turbidity were also not significantly different, therefore 194 kPa was used as best pressure. Flux increased from 35 to 72 $L.m^{-2}.h^{-1}$ by increasing crossflow velocity from 0.9 to 3.5 m/s. However, the highest crossflow velocity of 3.5 m/s gave lowest

TABLE 3.
HYDRAULIC RESISTANCE OF PARTICLE LAYER AS AFFECTED BY TRANSMEMBRANE PRESSURE, P_{tm} (0.1μm MEMBRANE PORE SIZE, CROSSFLOW VELOCITY 3.5 m/s, TEMP. 25°C)

Transmembrane pressure, P_{tm} kPa	Dynamic viscosity Cp	Flux l/m².h	$P_{tm}/J.\mu$	Hydraulic Resistance 1/m
194	1.214	65.62	$8.792x10^{12}$	$0.879x10^{13}$
137	1.183	58.78	$1.007x10^{13}$	$1.007x10^{13}$
93	1.193	47.90	$1.227x10^{13}$	$1.227x10^{13}$

TABLE 4.
HYDRAULIC RESISTANCE OF PARTICLE LAYER AS AFFECTED BY CROSSFLOW VELOCITY (0.1 μm MEMBRANE PORE SIZE, P_{tm} 194 kPa, TEMP. 25°C).

Crossflow velocity m/s	Dynamic viscosity Cp	Flux l/m².h	$P_{tm}/J\mu$	Hydraulic Resistance 1/m
3.5	1.152	72.49	8.479×10^{12}	0.848×10^{13}
2.2	1.151	45.98	1.324×10^{13}	1.324×10^{13}
0.9	1.137	35.14	1.755×10^{13}	1.755×10^{13}

permeate quality. The membrane resistance (R_m) were inversely proportional to membrane pore size. The hydraulic resistance (R_L) was inversely proportional to transmembrane pressure and crossflow velocity. Effect of R_L on flux was much higher than the effect of R_m within the range of pressures and velocities considered in this study.

LIST OF SYMBOLS

Jv	Volume flux, $(L.m^{-2}.h^{-1})$
R_m	Membrane Resistance, (m^{-1})
R_L	Hydraulic Resistance by Particle Layer, (m^{-1})
P_{tm}	Transmembrane Pressure, (kPa)
A	Area, (m^2)
V	Crossflow Velocity $(m.s^{-1})$
μ	Dynamic Viscosity of Feed, (Cp)

REFERENCES

BELLA, K. GIDEON, Z. and ZEKI, B. 1980. Orange Pectinesterase: Purification, Properties, and Effect on Cloud Stability. J. Food Sci. *45*, 1203.

BEVERIDGE, T. and HARRISON, J. E. 1986. Non-Enzymatic Browning in Pear Juice Concentrate at Elevated Temperatures. J. Food Sci. *10*, 1131.

BRUEMMER, J. H., BAKER, R. A. and ROE, B. 1976. Enzymes Affecting Flavor and Appearance of Citrus Product, Enzyme in Food and Beverage Processing. Robert, L. O. *et al.* Proceeding of Symposium.

CHERYAN, M. 1986. *Ultrafiltration Handbook*. Technomic Publishing Company, Lancaster, P.A.

DOESBURG, J. J. 1965. Pectic Substances in Fresh and Preserved Fruits and Vegetables, pp. 19 & 119. Institute for Research on Storage and Processing of Horticultural Produce, Wageningen, The Netherlands.

JENSON, G. and BOSSEN, C. E. 1984. Polarization Phenomena in Membrane Process. Synthetic Membrane Processes, Academic Press Inc.

KIRK, D. E., MONTROGOMERY, M. W. and KORTEKAAS, M. G. 1983. Clarification of Tangerine Orange Juice by Hollow Fiber Ultrafiltration. J. Food Sci. *48*, 1663.

LEE, M. S. and ATKINSON, T. 1985. Cross-Flow Microfiltration for Recovery of Intracellular Products. Process Biochem. *20*, 26.

LUND, D. B. 1977. Design of Thermal Processes for Maximizing Nutrient Retention. Food Technol. *31*, 71.

MEDINA, B. G. and GARCIA, A. 1988. Concentration of orange juice by reverse osmosis. J. Food Proc. Eng. *10*, 217.

NOVO FERMENT (SWITZERLAND) LTD. The Instruction Manual of PECTINEX ULTRA SP-L.

OWUSO, Y. J., MARSHALL, M. R., KOBURGER, J. A. and WEI, C. I. 1988. Low pH Inactivation of Pectinesterase in Single Strength Orange Juice. J. Food Sci. *53*, 504.

RAO, M. A., ACREE, T. E., COOLEY, H. J. and ENNIS, R. W. 1987. Clarification of Apple Juice by Hollow Fiber Ultrafiltration: Fluxes and Retention of Odor-Active Volatiles. J. Food Sci. *52*, 375.

YU, Z. R., CHIANG, B. H. and HWANG, L. S. 1986. Retention of Passion Fruit Juice Compounds by Ultrafiltration. J. Food Sci. *51*, 841.

GELATION KINETICS OF MEAT EMULSIONS CONTAINING VARIOUS FILLERS DURING COOKING

L. R. CORREIA[1]

Department of Agricultural Engineering
Technical University of Nova Scotia
P.O. Box 1000
Halifax, Nova Scotia, Canada, B3J 2X4

AND

G. S. MITTAL

School of Engineering
University of Guelph
Guelph, Ontario, Canada, N1G 2W1

Accepted for Publication February 13, 1991

ABSTRACT

A cylindrical shaped thermal scanning rigidity monitor (TSRM) was developed to determine shear rigidity modulus of meat batters during cooking. A meat fat-protein ratio of 1.8, moisture content of 62% and 8.6% filler were used. The fillers were buttermilk powder, corn starch, micro-crystalline cellulose, modified corn starch, modified wheat flour, soy-protein concentrate and whey-protein concentrate. Plots of rigidity modulus versus product-temperature showed two major thermal transitions. The first and most important transition (53 to 61°C) was due to myosin gelation. The second transition (64 to 69°C) was ascribed to the collagen softening. The maximum rigidity-temperature slopes of 0.60 to 1.02 kPa/°C occurred after the first transition.

INTRODUCTION

Heat induced gelation of muscle proteins is largely responsible for the physical and chemical stabilization of fat and water in comminuted red meat products (Ziegler and Acton 1984). The incorporation of fillers affect the gel formation

[1]Correspondence should be sent to: Dr. Lino R. Correia, Dept. of Agricultural Engineering, Technical University of Nova Scotia, P.O. Box 1000, Halifax, Nova Scotia, Canada, B3J 2X4

Journal of Food Process Engineering **14** (1991) 35–49. *All Rights Reserved.*

ability of sausage emulsion. The inclusion of ingredients which possess an ability to form gels could enhance gelation and contribute to the product hardness upon cooking. Thus, the gel forming ability is reflected by the kinetics of heat induced gelation of meat emulsion as a function of temperature. Shear modulus of rigidity reflects the gelation ability of meat emulsions.

Patana-Anake and Foegeding (1985) used a U-shaped thermal scanning rigidity monitor (TSRM) to obtain shear rigidity modulus of meat emulsions containing no filler or 3.5% soy protein concentrate or 3.5% vital wheat gluten. There was a sharp decline in the shear modulus in the 20 to 40°C range, attributable to fat melting. Above 55°C there was a very steep rise in shear modulus probably due to actomyosin gelation. Recently, continuous rigidity scanning was reported to be a more sensitive method for detecting sol-gel transformation transitions than batch techniques for protein systems (Hamann 1987).

Montejano *et al.* (1984) and Wu *et al.* (1985) also used U-shaped TSRM for turkey paste and meat emulsions, respectively. Wu *et al.* (1985) studied transitions occurring during the gelation of meat emulsion using a constant heating rate of 1°C/min. Three transition temperatures were observed at 38, 46 and 60°C, however, the formation of a rigid gel started at 46°C. Schweid and Toledo (1981) also reported transition points in meat batter to occur at 33 to 36°C and 57 to 67°C. They suggested that these temperatures represent the points where muscle proteins insolubilization and solubilization of collagen occur, respectively.

This paper describes kinetics of shear rigidity modulus of meat emulsion containing various fillers during cooking.

MATERIALS AND METHODS

Emulsion Preparation

On the basis of source material, functional properties and potential usage, the following fillers were selected. The numbers in brackets represent carbohydrate, protein, moisture and fat content in percentages, respectively: buttermilk powder (BMP) (44, 34, 5, 6), corn starch (CS) (90, 0, 10, 0), micro-crystalline cellulose (MCC) (94, 0, 6, 0), modified corn starch (MCS) (90, 0, 10, 0), modified wheat flour (MWF) (47, 45, 8, 0), soy-protein concentrate (SPC) (26, 67, 6, 0.5), and whey-protein concentrate (WPC) (53, 35, 4.5, 5). Compositions were provided by the manufacturers. Proximate compositions of the raw meat emulsions are given in Correia and Mittal (1990). It was based on the targeted meat protein level of 9.55%, meat fat-protein ratio of 1.8 and moisture content of 61.8% in the cooked product. The soluble spice mix contained 97% salt and $< 0.2\%$ glycerine, and nitrite source contained 83% salt, 8.3% sodium erythorbate, 6.4% sodium nitrite, 2% sodium carbonate, and $< 0.2\%$ glycerine. Total salt content was 2.38% in the raw meat emulsion, whereas the soluble spice level was

0.014%, and sodium nitrite level was 190 ppm. For 8 treatments (7 fillers and 1 control without filler) and 2 replications, the total number of experiments were 16. The process conditions were held constant.

Lean beef from one carcass was obtained from the University of Guelph Meat Lab., and pork back fat from a local meat plant. The lean beef and pork fat were each ground separately, through 9.5 mm and 12.7 mm diameter plates, respectively. The ground lean beef and pork fat were then packed in polyethylene bags and stored in a freezer at -18 ± 1°C. When required, these were thawed to 66 ± 1 h in a cooler at 2 ± 1°C, and then ground through a 6.4 mm plate. Fresh emulsions were prepared before each experiment. A batch of 1.5 kg raw meat emulsion was prepared using a smaller chopper (Eduard Mueller Gmbh, Type MTZ 10/70, W. Germany). The lean beef, salt, soluble spice and nitrite mix, and half the added ice were chopped at 13 rpm bowl speed for 10 revolutions. Then fat was added and chopped again for 10 revolutions. The filler (if any) and remainder of the ice were placed in the bowl and chopped again for 10 revolutions, then chopped for 130 revolutions at 25 rpm. A vacuum tumbler (Model 40; Lyco, Columbus, WI) was used to reduce the number of large air pockets in the emulsion. A vacuum of 50 kPa, tumbling speed of 18 rpm and time of 1.5 min were used.

Thermal Scanning Rigidity Monitor (TSRM) System

A shear rigidity modulus test was used to monitor gel formation process during cooking. A thermal scanning rigidity monitor (TSRM) was developed for this, and described below, which is a modification of Montejano *et al.* (1984) device.

The TSRM consisted of a base plate, inner and outer cylindrical water jacketed vessels, two sets of guides (top and bottom), a screw cap, guide studs (top and bottom) and rubber tubings. Figure 1 shows the cross-sectional view of the TSRM. The assembly process consisted screwing the inner water jacket to the base plate. The bottom and top guides were then placed on the base plate, and outer cylinder was placed on the guides. This created 8 mm gap between inner and outer cylinders. Meat batter was then inserted in the annular space with a spatula, up to 15 mm below the top of the outer cylinder. The outer cylinder cap was then screwed, as well as bottom guide stud.

An Instron universal testing machine (Model 4204; Instron Canada Ltd., Burlington, Ont.) with a 1 kN load cell was used to measure shear force. The base plate of the TSRM was fastened to the machine base, and top guide was attached to the load cell. The bottom and top guide studs were then removed.

A water bath (Model E3; Haake, Germany) recirculated water through the inner and outer cylinders to maintain uniform temperature in the meat emulsion. The temperature was increased at the rate of 0.66°C/min. T-type thermocouples were used to record various temperatures. The Instron machine was programmed to provide a cyclic vertical motion of the crosshead at a speed of 0.48 mm/min.

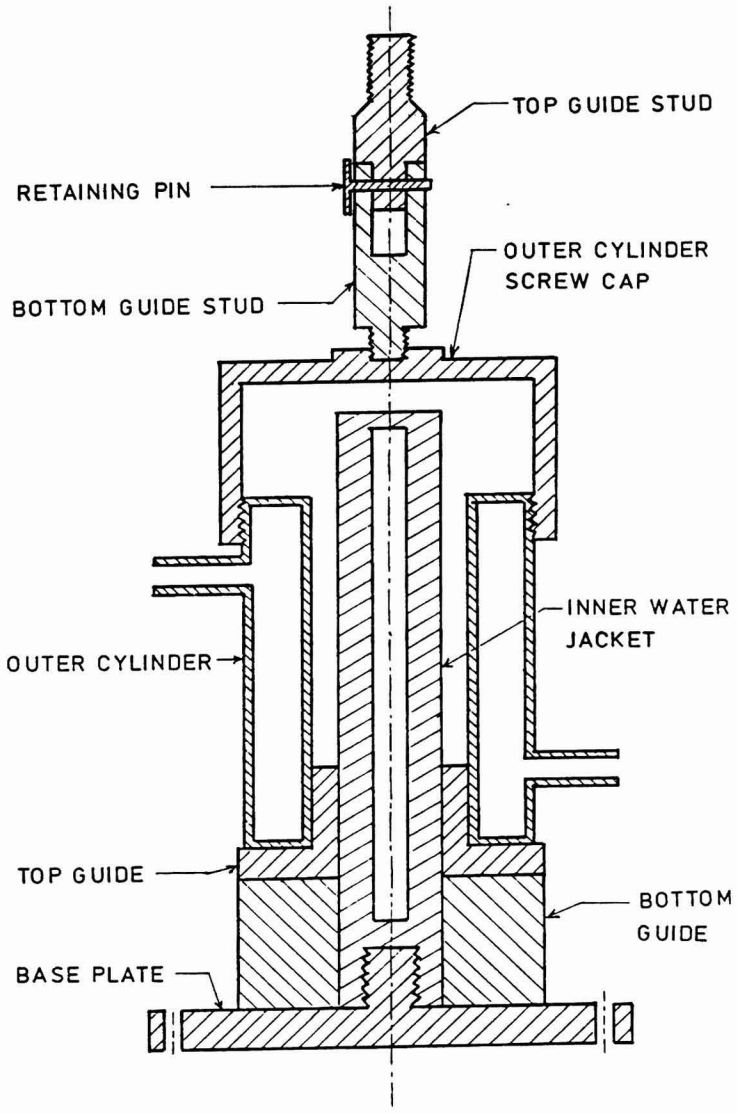

FIG. 1. CROSS-SECTIONAL VIEW OF THE THERMAL SCANNING RIGIDITY MONITOR APPARATUS

The amplitude was 0.24 mm, which provided a maximum shear strain of 3% and a cycle time of 2 min. The rigidity modulus was computed by (Correia 1988):

$$G = \frac{F}{2\,\pi.L.D}.\ln(R_2/R_1) \tag{1}$$

where G = modulus of rigidity, Pa; F = force amplitude, N; R_2 = inner radius of the outer cylinder, 0.023 m; R_1 = outer radius of the inner cylinder, 0.015 m; D = displacement amplitude, 0.00024 m, and L = average length of the sample, m.

Statistical Analyses

Statistical analyses of the data were conducted with either SAS on an IBM 4381 mainframe computer (SAS Institute, 1985a), or PC-SAS on an IBM-PC microcomputer (SAS Institute 1985b). For nonlinear regression analysis, the Nonlinear (NLIN) procedure of the SAS, with Gauss-Newton method and relative convergence criterion of 10^{-8}, was used. Other SAS procedures like ANOVA, for the analysis of variance and Duncan's multiple range test, and CORR, to compute univariate descriptive statistics and correlation, were used.

Kinetics Modelling

The change in modulus of rigidity (G) during cooking was modelled by the quadratic model:

$$G = C_1.T + C_2.T^2 \tag{2}$$

where c_1 and C_2 are constants.

Based on a reaction kinetics approach and Eyring's absolute reaction rate theory, the following model was developed (Correia and Mittal 1991):

$$\frac{dG}{dT} = \frac{k.T.(G_m - G_i)}{h.Q} \cdot \exp\left(\frac{\Delta S}{R_G} - \frac{\Delta H}{R_G.T}\right).(1 - X)^n \tag{3}$$

where T is product temperature, K, Q is the slope of product temperature versus time relationship, K/min, subscripts i and m denote initial and maximum G during cooking, R is the gas constant (8.314 kJ/(kg.mole)), K is the Boltzmann's constant (1.38E-23 J/K), h is the Planck's constant (6.625E-34J.s), ΔS is the entropy change of activation (kJ/(kg.mole.K)) and ΔH is the enthalpy change of activation (kJ/(kg.mole)). Thus ΔS, ΔH and n were calculated for all the properties changes of meat emulsions during cooking. The 'n' was found to be zero for all the properties changes.

Enthalpy-Entropy Compensation

Leffler and Grunwald (1963) reported the following linear relationship between ΔH and ΔS, known as enthalpy-entropy compensation:

$$\Delta H = T_c.\Delta S + B \tag{4}$$

where T_c is the isokinetic or isoequilibrium or compensation temperature (K) and B is a constant (kJ/(kg.mole)). Since ΔS is typically obtained using ΔH and ΔG (Gibbs free energy change), hence a linear plot of ΔH versus ΔS is not necessarily an evidence of enthalpy-entropy compensation (Petersen 1964). Krug *et al.* (1976) suggested the following two-step criteria to test this hypothesis:

(1) If enthalpy-entropy compensation arose from error propagation alone, then the null hypothesis, $T_{hm} = T_c$, would be accepted. T_{hm} (harmonic mean temperature) is defined by $N/(\sum_{i=1}^{N} /T_i)$, where N is the total number of different temperatures (T_i). However, if the thermodynamic compensation existed, then T_{hm} should not appear in 95% confidence interval (CI) for T_c.
(2) The correlation coefficient (r) be close to unity for both the ΔH versus ΔS relationship, as well as the ΔH versus ΔG relationship at T_{hm}.

These two criteria were used in our study to test the thermodynamic compensation.

RESULTS AND DISCUSSION

Shear rigidity modulus profiles

Plots of shear rigidity modulus (G) versus product-temperature for the control, BMP, SPC and WPC treatments; and CS, MCC, MCS and MWF treatments are shown in Fig. 2 and 3, respectively. Each point on the curve is the average of two replications. For all treatments the minimum and maximum G were 1.5 and 16 kPa, respectively, in the product-temperature range of 30 to 70°C. The G for meat emulsions of different compositions cooked in the same product-temperature range, reported by Patana-Anake and Foegeding (1985), Foegeding and Ramsey (1987), and Barbut and Mittal (1988), ranged from 4 to 17 kPa, 1 to 17 kPa, and 1 to 15 kPa, respectively. Thus, G values obtained in the present study are in the reported ranges. G was highly correlated ($Pr \leq 0.0001$, correlation coefficient (r) = 0.688, N = 486) with product-temperature. The replication effect was not significant at the 5% level, whereas both the filler and product-temperature effects were highly significant even at the 1% level. For all treatments, G was fairly constant up to the first thermal transition which occurred in the range 54 to 61°C. Schweid and Toledo (1981), Patana-Anake and Foegeding (1985), and Barbut and Mittal (1988) reported first thermal transitions, for meat emulsions of different compositions, at 57 to 67°C, 54 to 57°C and 54 to 58°C, respectively.

The first transition can be attributed to the gelation of myosin (Samejima *et al.* 1976). Yasui *et al.* (1979) and Ishioroshi *et al.* (1979) reported that the degree of myosin gelation reached a maximum between 60 to 70°C. Thus, the rigidity increase was due to partial myosin gelation. A second transition occurred between

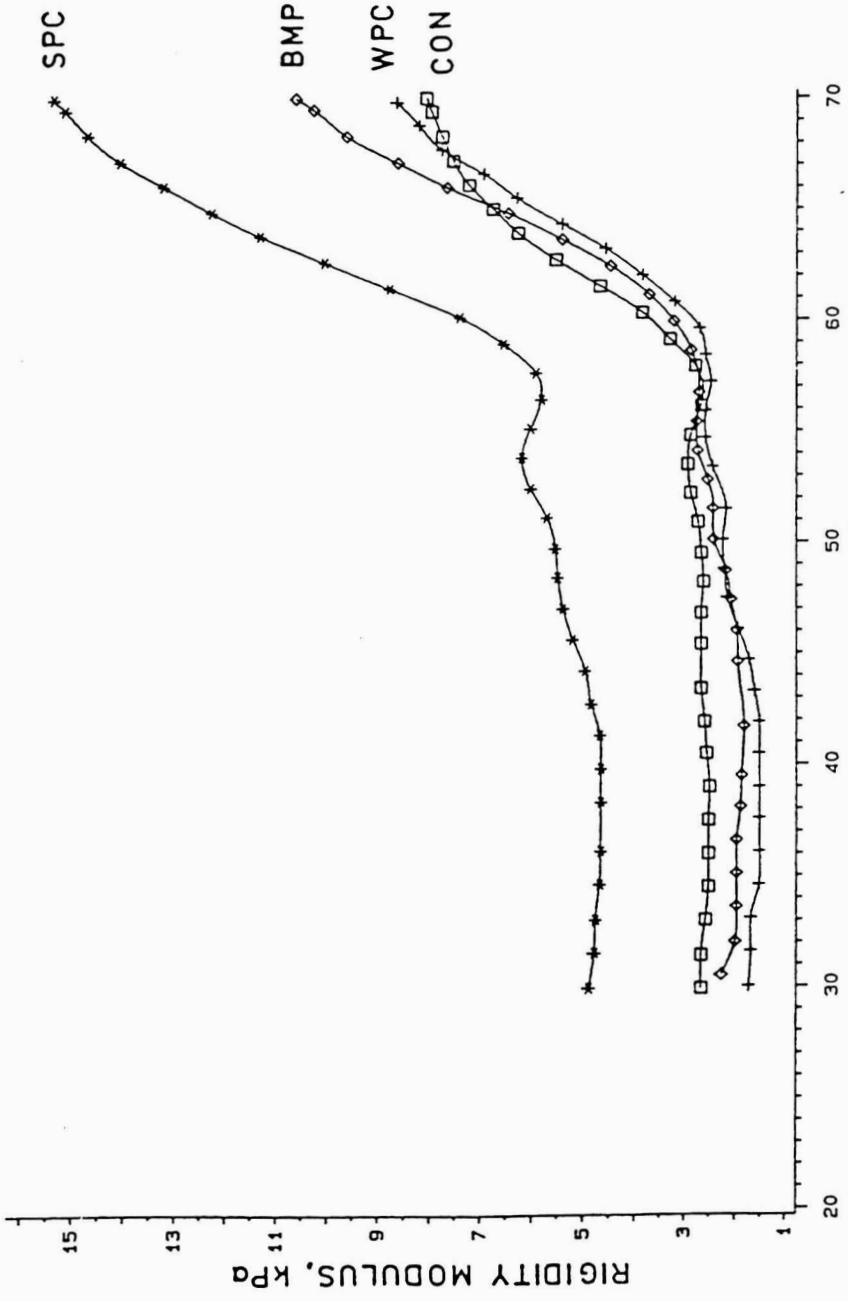

FIG. 2. PLOTS OF OBSERVED VALUES OF RIGIDITY MODULUS VERSUS PRODUCT-TEMPERATURE FOR THE CONTROL, BMP, SPC AND WPC TREATMENTS

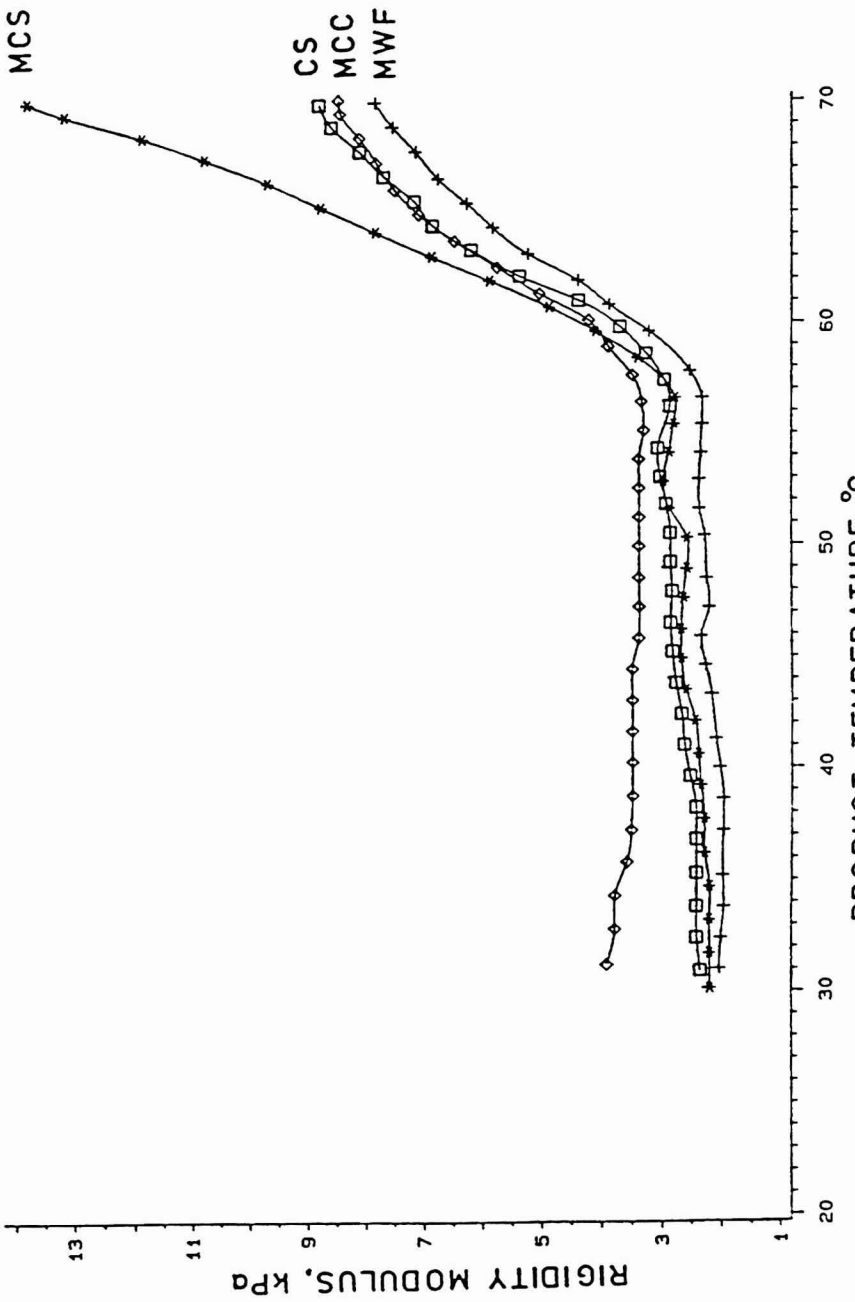

FIG. 3. PLOTS OF OBSERVED VALUES OF RIGIDITY MODULUS VERSUS PRODUCT-TEMPERATURE FOR THE CS, MCC, MCS AND MWF TREATMENTS

64 and 69°C for all treatments. Barbut and Mittal (1988) also obtained a transition between 59 and 69°C for poultry meat emulsions. This thermal transition is ascribed to the softening of collagen and sarcoplasmic proteins (Wright *et al.* 1977).

Up to the first transition the G values of SPC and MCC treatments were higher than 3 kPa, whereas the G values for the other treatments were lower than 3 kPa (Fig. 2 and 3). The insoluble solids of MCC and SPC fillers contributed to higher rigidity. The highly soluble WPC and BMP fillers accounted for lower rigidity.

Between the first transition and 70°C, the MCS and SPC treatments displayed the highest slopes of rigidity with respect to product-temperature (dG/dT). The cold water absorption (CWAF) of MCS, CS and MWF fillers were between 0.94 to 1.22. However, MCS treatment showed higher rigidity than CS and MWF treatments. The gel strength (GSF of the MCS, CS and MWF fillers were 5.38, 1.18 and 0.41 N, respectively. Thus, for fillers displaying similar CWAF, a higher GSF resulted in a higher G. Both the high CWAF and GSF of the SPC filler contributed to the high slope for the SPC treatment. Although the MCC filler demonstrated the highest CWAF (12.3), the rigidity was lower than that of the SPC treatment. The MCC filler could not form a firm gel when heated. Hence, the MCC treatment was less rigid than the SPC treatment. Above 64°C, the G for the BMP treatment increased more sharply than the WPC treatment (Fig. 2), possibly due to the whey-protein-casein-micelle-conglomerate. The slope (dG/dT) for the control treatment decreased after the second transition (64°C) indicating higher sensitivity to the softening of collagen and sarcoplasmic proteins. There was a highly significant correlation ($Pr \leq 0.0001$, $r = 0.972$, $N = 8$) between G and elastic modulus-2 (E_2) of meat emulsions (Correia 1988). The replication effect was not significant, whereas the filler effect was significant for G values at 70°C. Results of the Duncan's multiple range test, for filler effect are shown in Table 1. The SPC, MCS and BMP treatments provided significantly more rigid product than the control and MWF treatments. Patana-Anake and Foegeding (1985) found that rigidity modulus of meat emulsions containing vital wheat gluten were lower than corresponding values for the control treatment and the meat emulsion containing soy-protein concentrate. Thus, meat emulsions containing vital wheat gluten or modified wheat flour (which also contains some gluten) were less rigid compared to SPC treatment. There was no significant difference in G of the control and SPC treatments reported by Patana-Anake and Foegeding (1985), because of the lower level (3.5%) of filler compared to the higher level (8.55%) used in the present study.

Gelation Kinetics

The rigidity modulus temperature profile was modelled by the second-order polynomial between the first transition and 70°C (Table 2). Although a ramp

TABLE 1.
DUNCAN'S MULTIPLE RANGE TEST RESULTS FOR RIGIDITY MODULUS OF MEAT EMULSIONS COOKED TO 70°C CONTAINING DIFFERENT FILLERS

Filler	Rigidity modulus at 70°C (kPa)
CON	8.1 c*
BMP	10.6 b
CS	9.0 bc
MCC	8.4 bc
MCS	13.7 a
MWF	7.9 c
SPC	15.3 a
WPC	8.7 bc

* Means in the same column with identical letters are not significantly different at the 5 % level.

heat input was applied to the meat emulsions cooked in the thermal scanning rigidity monitor, the profile slope decreased slightly at higher temperatures, due to higher heat loss. Hence, the following quadratic equation was used to express product-temperature as a function of cooking-time.

$$T = P + Q.t + R.t^2 \quad (5)$$

where P, Q and R are constants. For all treatments P varied from 285 to 295 K, Q from 0.646 to 0.867 K/min and R from −0.66E-03 to −0.019 K/min^2. Plots (Fig. 4) of observed and predicted product-temperature as a function of cooking-time for the control treatment indicate the model's suitability.

The estimated ΔS and ΔH for G changes during cooking ranged from −337 to −299 kJ/(kg.mole.K), and −10732 to 1896 kJ/(kg.mole), respectively (Table 3). The range of values of the ratio of standard error to estimated error of ΔS and ΔH were 0.04 to 0.63%, and 3.06 to 9.38%, respectively. Although the ΔH for all treatments, except the MWF treatment were negative, the ΔG values were positive for all treatments indicating that thermal energy was required for changes in ΔG. A decrease in entropy occurred during gelation. Aggregation into an ordered state was apparently responsible for the lower entropy at the activated state.

TABLE 2.
REGRESSION MODELS OF RIGIDITY MODULUS (G) AS A FUNCTION OF TEMPERATURE DURING COOKING

Filler	Parameters			
	C_1*		C_2	
	Estimate	SE	Estimate	SE
CON	-4.40E-01	3.49E-02	1.36E-04	1.03E-04
BMP	-7.83E-01	1.99E-02	2.37E-03	5.86E-05
CS	-4.67E-01	3.15E-02	1.44E-03	9.31E-05
MCC	-4.07E-01	3.25E-02	1.26E-03	9.62E-05
MCS	-8.73E-01	1.98E-02	2.66E-03	5.86E-05
MWF	-4.01E-01	2.26E-02	1.24E-03	6.68E-05
SPC	-7.56E-01	4.47E-02	2.34E-03	1.32E-04
WPC	-5.98E-01	1.95E-02	1.82E-03	5.77E-05

*$G = C_1 T + C_2 T^2$; SE = standard error of estimate; Degrees of freedom for error = 6 to 8; Pr > F was 0.0001; and coefficient of determination (R^2) ≥ 0.997.

Regression parameters of a hypothetical linear enthalpy-entropy relationship for G changes during cooking were T_c = 334 K and B = 101598 kJ/(kg.mole) (R^2 = 0.982, Pr > F was 0.0001). The 95% CI of T_c, 288 to 380 K, included the T_{hm} value of 326 K. Hence, the first criterion of enthalpy-entropy compensation was not satisfied.

CONCLUSIONS

The thermal scanning rigidity monitor (TSRM) was able to measure the meat emulsion gelation process. For all treatments, the rigidity modulus (G) was fairly constant up to about 55 to 58°C. Above this transition there was a sharp increase in the rigidity. The first thermal transition occurred in the range of 54 to 61°C and the second between 64 and 69°C. The reaction kinetics approach was suitable to determine enthalpy and entropy of activation for G changes during cooking. The kinetics parameters reflected the filler effects. The reaction rate constant was zero, the Gibbs free energy of activation was positive and the entropy change of activation was negative, indicating the need for thermal energy for G changes.

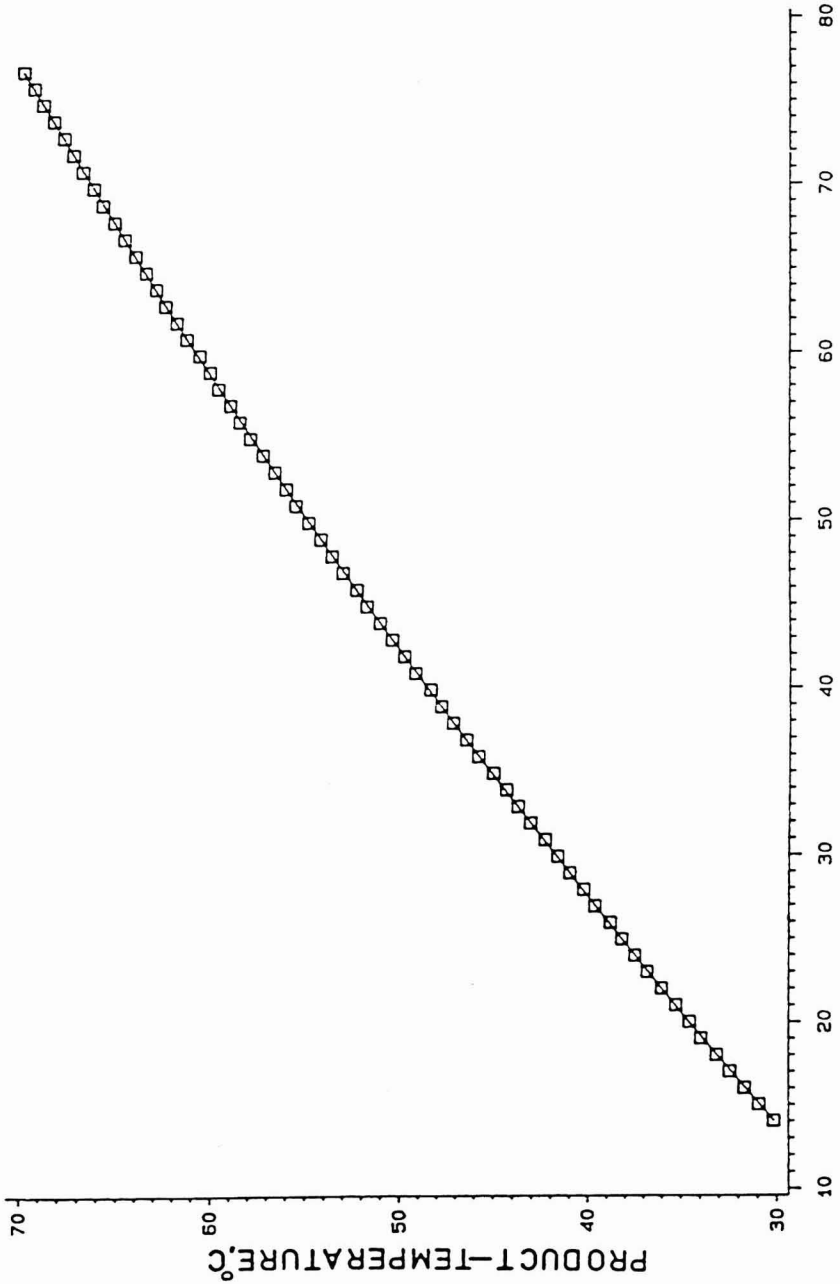

FIG. 4. PLOTS OF OBSERVED AND PREDICTED PRODUCT-TEMPERATURES FOR THE FIRST REPLICATE OF THE CONTROL TREATMENT DURING COOKING IN A THERMAL SCANNING RIGIDITY MONITOR

TABLE 3.
KINETIC PARAMETERS OF SHEAR RIGIDITY MODULUS (G) CHANGES DURING COOKING

Filler	Kinetic parameters*			
	ΔS kJ/(kg.mole.K)		ΔH kJ/(kg.mole)	
	Estimate	SE	Estimate	SE
CON	-333	1.69	-9886	570
BMP	-323	1.92	-6940	651
CS	-336	2.11	-10215	716
MCC	-324	1.78	-7770	585
MCS	-337	1.71	-10732	579
MWF	-299	0.13	1896	58
SPC	-331	1.72	-9011	583
WPC	-333	1.59	-9836	537

* Degrees of freedom for error = 6 to 8;
Mean sum of squares of error ≤ 4.02E-06.

SPC and MCS treatments provided more rigid product due to the ability of the fillers to form strong gels in water. The BMP treatment provided significantly more rigid product than in the control and MWF. The ability of polysaccharides and proteins, present in the fillers, to form firm and resilient gels contributed to the formation of a more rigid meat emulsion at 70°C. Greater water absorption and emulsifying ability of the fillers formed more rigid meat emulsion.

ACKNOWLEDGMENTS

The research was supported by the Natural Science and Engineering Research Council of Canada and the Ontario Ministry of Agriculture and Food.

REFERENCES

BARBUT, S. and MITTAL, G. S. 1988. Rheological and gelation properties of meat batters prepared with three chloride salts. J. Food Sci. *53*, 1296–1299, 1311.

CORREIA, L. R. 1988. Selection Criteria of Meat Emulsion Fillers Based On Cooking Kinetics in a Smokehouse. Ph.D. thesis, University of Guelph, Guelph, Ontario, Canada.

CORREIA, L. R. and MITTAL, G. S. 1990. Stress relaxation kinetics of meat batters containing various fillers during smokehouse cooking. J. of Texture Studies *21*, 75–96.

CORREIA, L. R. and MITTAL, G. S. 1991. Kinetics of hydration properties of meat emulsions containing various fillers during smokehouse cooking. Meat Sci. *29*, 335–351.

FOEGEDING, E. A. and RAMSEY, S. R. 1987. Rheological and waterholding properties of gelled meat batters containing iota carrageenan, kappa carrageenan or xanthan gum. J. Food Sci. *53*, 549–553.

HAMANN, D. D. 1987. Methods for measurement of rheological changes during thermally induced gelation of proteins. Food Technol. *41*(3), 100–108.

ISHIOROSHI, M., SAMEJIMA, K. and YASUI, T. 1979. Heat induced gelation of myosin: factors of pH and salt concentrations. J. Food Sci. *44*, 1280–1284.

KRUG, R. R., HUNTER, W. G. and GRIEGER, R. A. 1976. Enthalpy-entropy compensation. 2. Separation of chemical from statistical effect. J. Phy. Chem. *80*, 2341–2351.

LEFFLER, J. E. and GRUNWALD, E. 1963. *Rates and Equilibria of Organic Reactions*. pp. 128–314, John Wiley & Sons, New York.

MONTEJANO, J. G., HAMANN, D. D. and LANIER, T. C. 1984. Thermally induced gelation of selected comminuted muscle systems—rheological changes during processing, final strengths and microstructure. J. Food Sci. *49*, 1496–1505.

PATANA-ANAKE, C. and FOEGEDING, E. A. 1985. Rheological and stability transitions in meat batters containing soy protein concentrate and vital wheat gluten. J. Food Sci. *50*, 160–164.

PETERSEN, R. C. 1964. The linear relationship between enthalpy and entropy of activation. J. Org. Chem. *29*, 3133–3135.

SAMEJIMA, K., TAKAHASHI, K. and YASUI, T. 1976. Heat-induced denaturation of myosin total rod. Agric. Biol. Chem. *40*, 2455–2464.

SAS INSTITUTE INC. 1985a. *SAS User's Guide: Statistics*, Version 5 Edition. Cary, NC.

SAS INSTITUTE INC. 1985b. *SAS/STAT Guide for Personal Computers*, Version 6 Edition, Cary, NC.

SCHWEID, J. M. and TOLEDO, R. T. 1981. Changes in physical properties of meat emulsion batters during cooking during heating. J. Food Sci. *46*, 850–855, 859.

WRIGHT, D. J., LEACH, I. B. and WILDING, P. 1977. Differential scanning calorimeter studies of muscle and its constituent proteins. J. Sci. Food Agric. *28*, 557–564.

WU, M. C., LANIER, T. C. and HAMANN, D. D. 1985. Rigidity and viscosity changes of croaker actomyosin during thermal gelation. J. Food Sci. *50*, 14–19, 25.

YASUI, T., ISHIOROSHI, M., NAKANO, H. and SAMEJIMA, K. 1979. Changes in shear modulus, ultrastructure and spin-spin relaxation times of water associated with heat-induced gelation of myosin. J. Food Sci. *44*, 1201–1204, 1211.

ZIEGLER, G. R. and ACTON, J. C. 1984. Mechanisms of gel formation by proteins of muscle tissue. Food Technol. *38*(5), 77–82.

MATHEMATICAL MODELLING OF RICE BRAN OIL EXPRESSION

K. SIVALA[1]

Post Harvest Technology Centre, Indian Institute of Technology, Kharagpur—721 302, India

and

V. VASUDEVA RAO and S. SARANGI

Cryogenic Engineering Centre, Indian Institute of Technology, Kharagpur—721 302, India

and

R. K. MUKHERJEE and N. G. BHOLE

Post Harvest Technology Centre, Indian Institute of Technology, Kharagpur—721 302, India

Accepted for Publication December 13, 1990

ABSTRACT

The expression of liquid from a solid-liquid matrix of oil-bearing material is a complex process and is incompletely understood. An investigation was taken up to understand the phenomena relating to compression and consolidation of rice bran and gain an insight into the flow behavior of oil under uniaxial compression. A mathematical model based on one-dimensional consolidation theory (Terzaghi 1943) was developed with suitable assumptions, taking into account the test-cell geometry. The experiments were conducted with two types of parboiled rice bran; original unsieved bran and bran sieved through B.S. 30 mesh. The developed model was tested and a close agreement was found between calculated and observed values.

INTRODUCTION

Rice bran is a by-product of rice milling obtained during polishing of brown rice. It accounts for 5–8% by weight of rough rice milled. The oil content in parboiled bran varies from 20–28% by weight.

[1]Correspondence should be send to: Dr. K. Sivala.

Journal of Food Process Engineering **14** (1991) 51–68.

In India, rice bran oil is obtained by the solvent extraction process only and mostly industrial grade oil is produced due to the high free fatty acid (FFA) content in the bran due to the hot and humid conditions of storage favoring lipolysis. One obvious way out of this would be to extract the oil from the bran immediately after production so that it is usable for edible purposes. However, due to the scattered location of rice mills in the villages and of solvent extraction plants in towns, the bran has to be transported over long distances to reach the extraction plants. This deteriorates the quality and at the same time increases the cost of raw material and hence the price of the finished product, the oil.

Mechanical pressing of rice bran seems to be promising for the organised sector of rice mills for immediate extraction of oil. Besides, oil obtained by this method is of better quality and requires only limited refining. However, almost nothing is known about the technology of hydraulic pressing of rice bran for oil expression. The available literature on this subject, apart from being scanty, does not cover the engineering aspects of the process at all. Before embarking on the development of a technology for mechanical expression of oil from bran, an attempt was therefore made to explain the concepts of compression and consolidation of rice bran leading to the expression of oil. A mathematical model based on Terzaghi's one-dimensional consolidation theory was developed with suitable assumptions. Experiments were conducted with the developed rice bran oil expression unit. The model so developed adequately describes the process, giving an insight into the nature of flow of oil from rice bran under uniaxial compression.

When brown rice is subjected to polishing, the pericarp, the tegmen or seed coat and the aleurone cells are removed. Some aleurone cells which contain oil bodies are ruptured to spill the oil bodies (Fig. 1). On application of pressure, the ruptured cells get compressed and more oil bodies are released.

CONCEPT OF EXPRESSION OF RICE BRAN OIL

Expression is a process of separation of liquid from a two-phase solid-liquid system by compression under conditions that permit the liquid to escape, while the solid is retained between the compressing surfaces.

The resistance to the flow of liquid through the voids in a bed of solids is the resultant of the total drag. The flow of liquid through the tortuous channels of the porous mass of biological origin is a complex process. It may be assumed that the actual channels are replaced by parallel conducts, each of variable cross section and that the difference in hydraulic radius of each channel is adequate to account for the variation in channel cross-sectional size and shape (McCabe and Smith 1967).

Physical phenomenon of expression process could be visualized from the work of Gurnham and Masson (1946), who had conducted experiments with synthetic

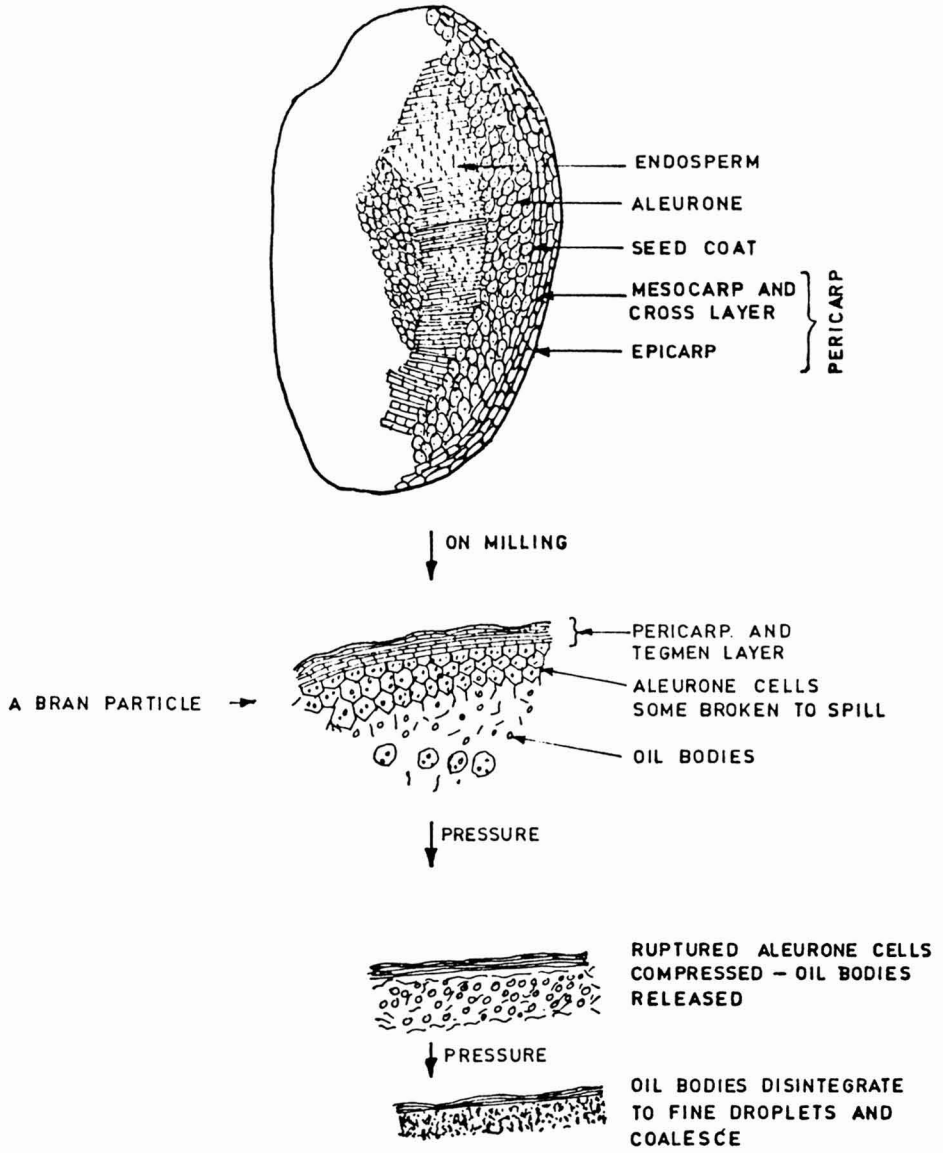

FIG. 1. SCHEMATIC FLOW SHEET FOR RUPTURE OF ALEURONE CELLS DURING POLISHING FOLLOWED BY RELEASE AND DISINTEGRATION OF OIL BODIES UNDER PRESSURE

mixtures of solids and liquids. The reduction in volume of compressible material may be due to deformation of solid particles (bending or flattening), slipping of the particles, thus total void space decreases under the influence of applied pressure. With further compression, the load is transferred to liquid phase and

if flow channels are available in the solid matrix, the liquid will move outside of the system. The removal of liquid from the system will relieve a part of the applied pressure and the load is gradually shifted to the solid phase. Thus the process of compression continues till equilibrium stage is reached, when the flow of the liquid to outside of the system stops.

Schewartzberg *et al.* 1982 have reported that the compaction pressure has basically three components: Solid compressive in the press cake, the pressure exerted by the fluid in press cake pores (voids) and the stress component corresponding to the friction force developed between the press cake and the wall surrounding. If cake length to diameter ratio is less than 0.6, the effect of frictional stress would be negligible. In general these stresses are interrelated by differential and integral force balances. The nature of these force balances depend on the press cake geometry, the pressing surface motion and the fluid flow path, where the outflow occurs through a cake-retaining filter medium at the bottom of the test-cell. Further it was reported that the complexity of the flow paths and solid motion in the vicinity of the nip, it is difficult to translate these results into analytically useful data. It is also stated that expression in some respects is compared with filtration. In compressible filter cakes, flow, induced pressure drop causes increased cake compaction in the down stream direction leading to flow resistance. As a result quite large pressure drops may be needed to sustain a given rate of flow.

At the beginning of compression, rice bran as a material represents a three-phase system: air, oil and solid bran particles. In the initial stage of compression, rearrangement of the oil bearing bran particles causes a decrease in the volume of interparticle voids of the bed. This may be due to escape of entrapped air. As compression proceeds, individual oil bearing bran particles start getting squeezed into the interparticle voids with an accompanying loss in their initial geometry. At this stage, the decrease in volume is mainly due to the deformation of particles. With further compression, a stage is soon reached when the intercellular structure of the oil bearing bran particles break releasing the oil into the surrounding voids. At this stage the sample represents a saturated two-phase system consisting of incompressible deoiled bran particles forming a cake matrix and a liquid phase consisting of the incompressible oil contained in the voids of the former. Under these conditions, the applied pressure is shared by the solid mass (deoiled bran particles) and the oil filled in the surrounding voids.

APPLICATION OF CONSOLIDATION THEORY FOR OIL EXPRESSION

Several research workers have used Terzaghi's one-dimensional consolidation theory to explain the liquid expression process in different materials having a two-phase system of solid and liquid.

In treating consolidation Shirato *et al.* (1970) have used various improved forms of Terzghi's theory and calculated internal flow from slurries and compactible beds of particles which are individually incompressible but deformable enough to accommodated bed compaction.

Schwartzberg *et al.* (1977) have reported that most expression process involving cellular matter deal with a particulated bed which initially contains little or no interstitial fluid. The bed must undergo compaction before the interparticle voids fill up with the fluid. The fluid emanates from the interior of the particles which therefore must be both deformable and compressible.

Mrema and McNulty (1985) have developed a mathematical model of mechanical oil expression from oilseeds (rapeseed and cashew) based on Terzaghi's theory for the consolidation process of a saturated medium (oil cake). The model has been successfully applied to experimental data, which revealed that the flow of oil across cell wall in the seed kernel was the rate determining step.

Singh and Singh (1987) have reported a mathematical model correlating various governing parameters explaining the rapeseed oil expression process. They considered radial movement of oil under uniaxial compression process. Further, it was stated that the experimental and predicted data on time variation of oil expressed were in close agreement with each other.

EXPERIMENTAL PROCEDURE

The experiments were conducted with parboiled rice bran obtained from a commercial rice mill. The bran was obtained by passing brown rice through three successive abrasive type polishers (SCHULE TYPE). Parboiling of paddy causes the bran to adhere to the endosperm firmly. Therefore, during polishing, along with brown rice 10 percent paddy was also added to act as abrasive surface for better polish. Due to this fact, bran obtained contained ground husk particles, most of which are larger than 0.5 mm diameter.

BRAN PARTICLE SIZE

The bran particle size distribution was determined by differential sieve analysis. A Vibratory-type mechanical sieve shaker (Rotap machine) was used. A bran sample of 200 g was placed on the top sieve and shaken for 20 min. The particle size distribution is presented in Table 1. The fraction retained on BS Sieve No. 30 constituted 18.25% husk particles. The mass mean diameter, the arithmatic mean diameter and volume surface mean diameter of the particles were found to be 0.029, 0.025 and 0.207 cm, respectively.

TABLE 1.
DIFFERENTIAL SIEVE ANALYSIS OF PARBOILED RICE BRAN

Sample size — 200 g
Moisture content — 7.2% (wb)
Shape factor — 1.4

B.S. Mesh No.	Mesh size D_{pi} (cm)	Average opening $\bar{D}_i$ (cm)	Weight fraction $\Delta\emptyset_i$	$\frac{\Delta\emptyset_i}{\bar{D}_i}$	No. of particles per g $N_i = \frac{1}{a\,\rho_p}\frac{\Delta\emptyset_i}{\bar{D}_i^3}$	$N_i\bar{D}_i$ (cm)	$\Delta\emptyset_i\bar{D}_i$ (cm)
25/30	0.060/0.050	0.0550	0.0625	1.136	321.02	17.656	3.437×10^{-3}
30/36	0.050/0.042	0.0460	0.1200	2.608	1053.72	48.471	5.520×10^{-3}
36/60	0.042/0.025	0.0335	0.1625	4.850	3694.34	123.760	5.443×10^{-3}
60/72	0.025/0.021	0.0230	0.6050	26.304	42499.71	997.493	0.139×10^{-1}
72/85	0.021/0.018	0.0195	0.0500	2.564	5763.47	131.493	9.750×10^{-4}
85/100	0.018/0.015	0.0165	-	-	-	-	
Pan	-	-	-	-	-	-	
			1.0000	37.462	53332.26	1318.87	0.02929

Shape constant, a = 0.9; Particle density, $\rho_p = 1.30$ g/cm^3

EXPERIMENTAL

Each 100 g bran sample was subjected to five levels of applied pressure (72.3, 120, 190, 260 and 307.7 kg/cm^2) for a duration of 45 min. A dial gauge was placed to read change in bran height with an accuracy of 0.01 mm. Simultaneously oil yield (mL) was measured at one-minute interval. The experiments were conducted thrice for each level of applied pressure. Average of experimental values are plotted (Fig. 3 through Fig. 7). The standard deviation (SD), standard error (SE) and coefficient of variation (COV) were calculated and shown in the respective figures.

The weighed bran sample was poured into the test-cell and was placed concentrically on the hydraulic press. The load was applied gradually up to the desired level and maintained constant for 45 min. The expressed oil was collected in a graduated test tube of 0.1 accuracy.

DEVELOPMENT OF THE GOVERNING EQUATION FOR RICE BRAN OIL EXPRESSION

The following assumptions are made in developing the equation:

(1) The bran cake is a homogenous phase and is saturated with oil.
(2) It is a two-phase system consisting of solid bran particles and oil.
(3) The cake matrix which forms the solid phase consists of compressible solid particles.
(4) The liquid phase consists of an incompressible oil.
(5) Darcy's law is valid for flow of oil through the porous mass of cake.
(6) Deformation is due to change in particle volume and occurs only in the direction of load.
(7) Oil drains out and moves only in the vertical direction due to gravitational force and the applied load, confining the flow laterally.
(8) The boundary is a free surface offering no resistance to the flow of oil.
(9) The change in thickness of the bran cake matrix during consolidation is insignificant.
(10) Under constant load, the coefficients of consolidation and permeability are constant.

The expression of rice bran oil cannot be taken as a simple compression or consolidation process; instead, it can be treated as a two-stage process consisting of compression till the voids are filled with oil followed by consolidation after it attains a two-phase system: bran and oil.

Consolidation process of rice bran under uniaxial compression is analogous to the consolidation of waterlogged soils. Therefore, theories and differential equations developed in soil mechanics (Terzaghi 1943; Punmia 1983 and Murthy 1984) have been adopted to describe and correlate constant pressure expression.

The fundamental differential equation governing flow through the saturated two-phase system can be adopted in case of rice bran for oil flow, as given below;

$$\frac{\partial u}{\partial t} = C_o \frac{\partial^2 u}{\partial z^2} \tag{1}$$

i.e., the rate of change of pore liquid pressure is proportional to the change in hydraulic pressure gradient.

The solution of the above equation is accomplished by means of Fourier series (Punmia 1983) under the defined boundary conditions of the test-cell geometry (Fig. 2).

During the process of primary consolidation, the rate of oil yield is proportional to the hydraulic gradient i.e., d_Q/dt is proportional to $\partial u/\partial z$.

Therefore, the cumulative oil yield (Q) at any time (t) is given by

$$Q = \int_o^t \frac{\partial u}{\partial z} dt \tag{2}$$

Hence the problem is to find the solution of u(Z,t) of Eq. (1) and obtain oil yield Q(t), from $\frac{\partial u}{\partial z}|_{z=0}$ as a function of time t. By solving Eq. (1) and (2), the final equation is derived. The calculated values Q(cal) and the observed values Q(obs) are to be compared at any time (t).

Solution of the Differential Equation

The fundamental equation governing the oil flow is obtained from Eq. (1).

$$\frac{\partial u}{\partial t} = C_o \frac{\partial^2 u}{\partial z^2} \quad \text{with boundary conditions}$$

at $z = H$, $\frac{\partial}{\partial z} = 0$

at $z = O$, $u = 0$

BOUNDARY CONDITIONS

at $z = 0$, $u = 0$

at $z = H$, $\frac{\partial u}{\partial z} = 0$

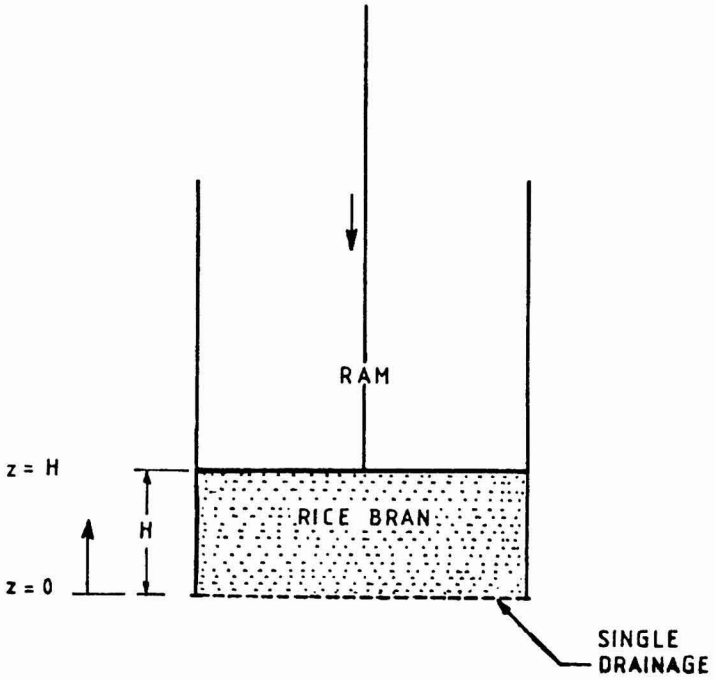

FIG. 2. CONSOLIDATION PROCESS FOR RICE BRAN OIL EXPRESSION

where C_o is the coefficient of consolidation. In terms of nondimensional variables Eq. (1) could also be written as:

$$\frac{\partial U}{\partial \tau} = \frac{\partial^2 U}{\partial \xi^2} \tag{3}$$

where $U = u/u_o$

$\xi = z/H$

and $\tau = c_o t/H^2$

The solution of the differential Eq. (3) governing the oil flow is obtained by means of Fourier series. The solution must satisfy the following initial and boundary conditions (Fig. 2)

$$U = 1, \quad \text{at} \quad \tau = 0$$
$$U = 0, \quad \text{at} \quad \xi = 0$$
$$\frac{\partial U}{\partial \xi} = 0, \quad \text{at} \quad \xi = 1$$

$$\left.\frac{\partial U}{\partial \xi}\right|_{\xi=o} = 2 \sum_{n=o}^{\infty} \exp\left(-\frac{(2n+1)^2\pi^2\tau}{4}\right) \tag{4}$$

We can relate the accumulated oil yield Q, as a function of time using the time integral of $\frac{\partial U}{\partial \xi}|_{\xi=0}$ from t = o to t = t with a proportionality constant (K), which describes the oil cake properties.

$$Q = K'' \int_o^t \left.\frac{\partial u}{\partial z}\right|_{z=o} dt = K' \int_o^{\tau} \left.\frac{\partial U}{\partial \xi}\right|_{\xi=o} d\tau \tag{5}$$

$$= 2K' \sum_{n=o}^{\infty} \int_o^{\tau} \exp\left(-\frac{(2n+1)^2\pi^2\tau}{4}\right) d\tau \tag{6}$$

Substituting Eq. (4) in Eq. (5) and on simplification, we get

$$Q = K\left[1\left(1 - e^{-(\pi^2/4)\tau}\right) + \frac{1}{9}\left(1 - e^{-(9\pi^2/4)\tau}\right) + \ldots\right] \tag{7}$$

Neglecting higher terms,

$$Q = K\left(1 - e^{-(\pi^2\tau/4)}\right) \tag{8}$$

or,

$$Q_{sat} = K\left(1 - e^{-\beta t}\right) \tag{9}$$

where $\tau = C_o t/H^2$ and hence $\beta = (\pi^2 C_o)/(4H^2)$,
K describes rice bran oil cake properties,
C_o coefficient of consolidation, cm^2/s,
H rice bran bed height under consolidation process, cm.

From theory we evaluate the integral for known time, 't'. Taking the oil yield for that time (t) from experimental results, we calculate K. Subsequently using this K value and β value at different times we evaluate the integral (Eq. 5) to obtain the oil yield as a function of time.

The application and validity of the above mathematical model are verified by using the experimental data obtained from the bran oil expression by hydraulic pressing.

VERIFICATION OF THE MATHEMATICAL MODEL

In the developed mathematical model, the value of β was so chosen as to obtain the least variation in Q(cal) and Q(obs) for each set of data at each constant applied pressure. The constant K has the same unit of oil yield and it was assumed that the value of Q saturated be equal to K at the end of 45 min at a given constant pressure. The values of K and β are tabulated for unsieved and sieved bran respectively in Table 2.

The values of Q(cal) and Q(obs) are shown in Fig. 3 through 7, comparing oil yield from unsieved and sieved bran at each level of applied pressure. The

TABLE 2.
CONSTANTS K AND β USED IN THE VERIFICATION OF THE MATHEMATICAL MODEL

Type of bran	Applied pressure (kg/cm^2)	K (ml)	β (min^{-1})
Unsieved	72.26	4.4	0.06641433
	120.00	6.7	0.07084172
	190.00	9.5	0.05735546
	260.00	11.1	0.07415410
	307.74	9.0	0.09316871
Sieved	72.26	7.6	0.07111696
	120.00	8.9	0.06969139
	190.00	6.0	0.05972532
	260.00	10.1	0.06141772
	307.74	11.7	0.06429869

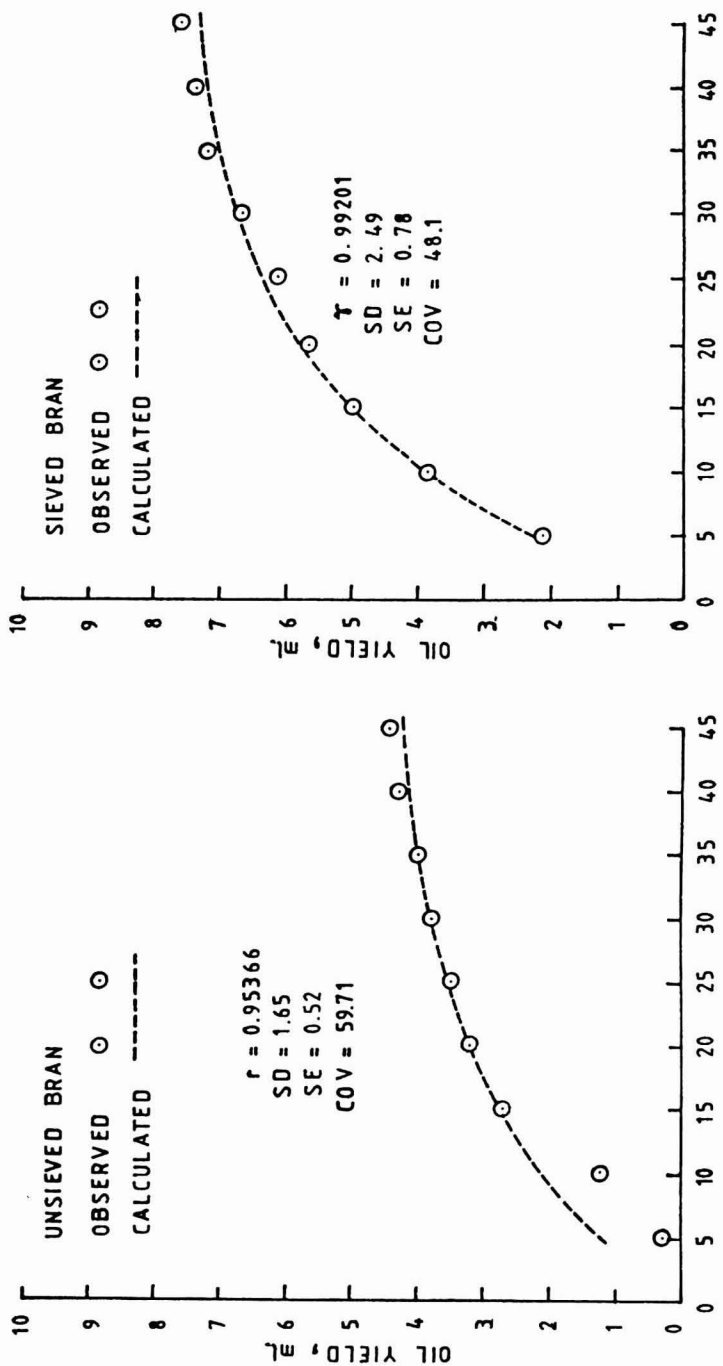

FIG. 3. EFFECT OF PRESSING TIME ON OIL YIELD AT 72.26 kg/cm^2

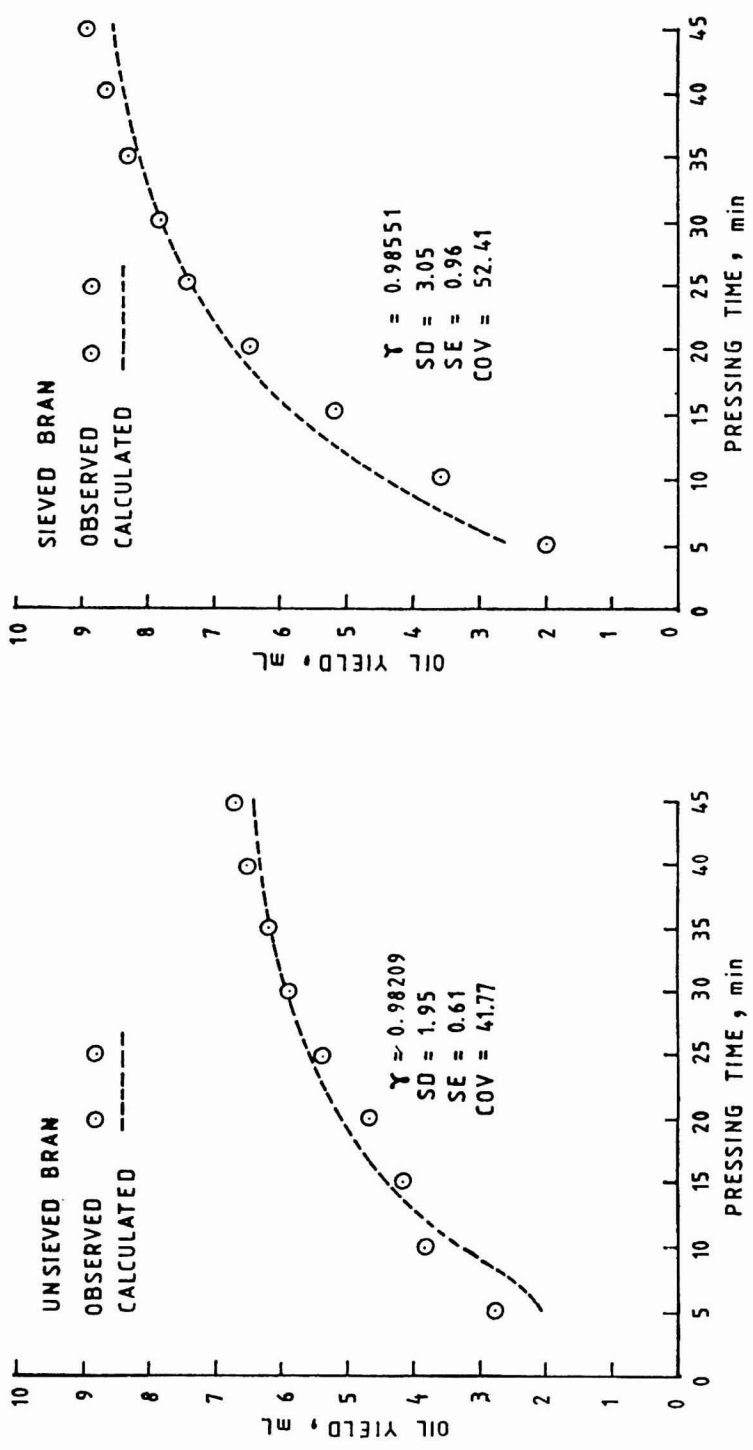

FIG. 4. EFFECT OF PRESSING TIME ON OIL YIELD AT 120 kg/cm^2

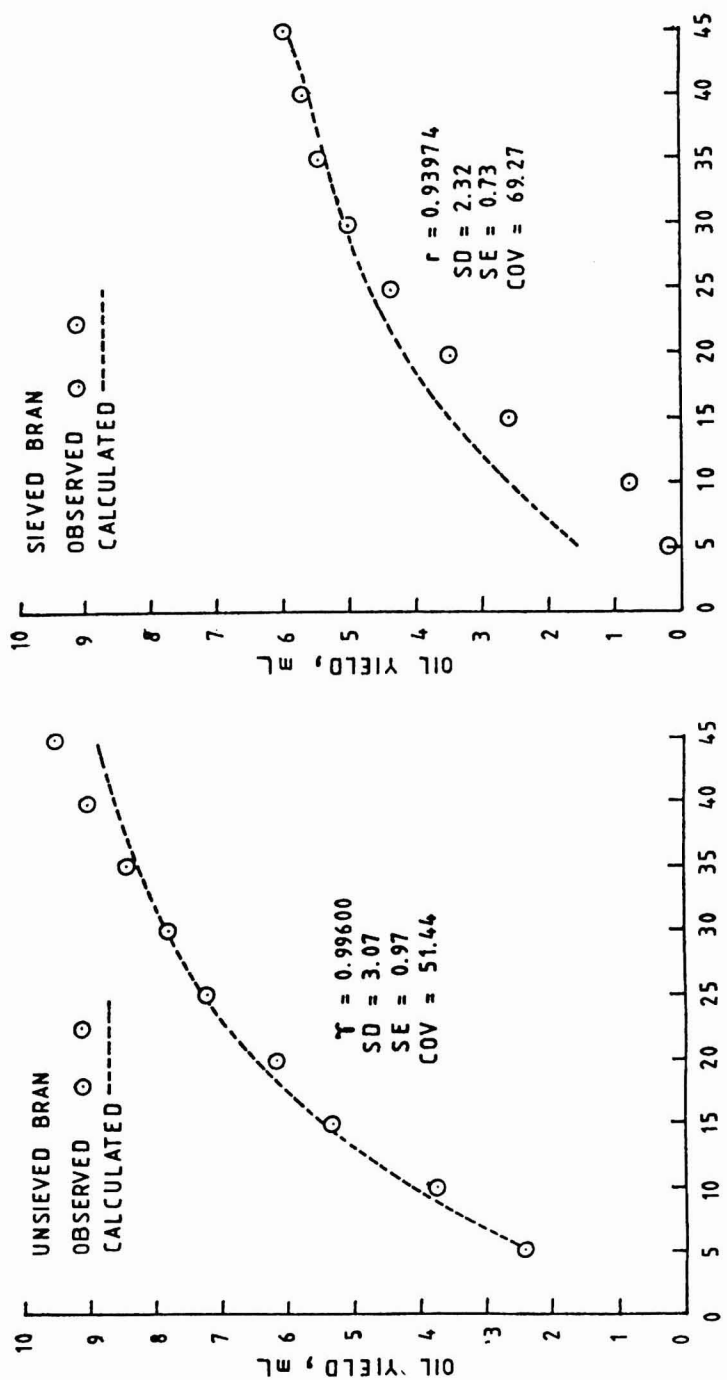

FIG. 5. EFFECT OF PRESSING TIME ON OIL YIELD AT 190 kg/cm^2

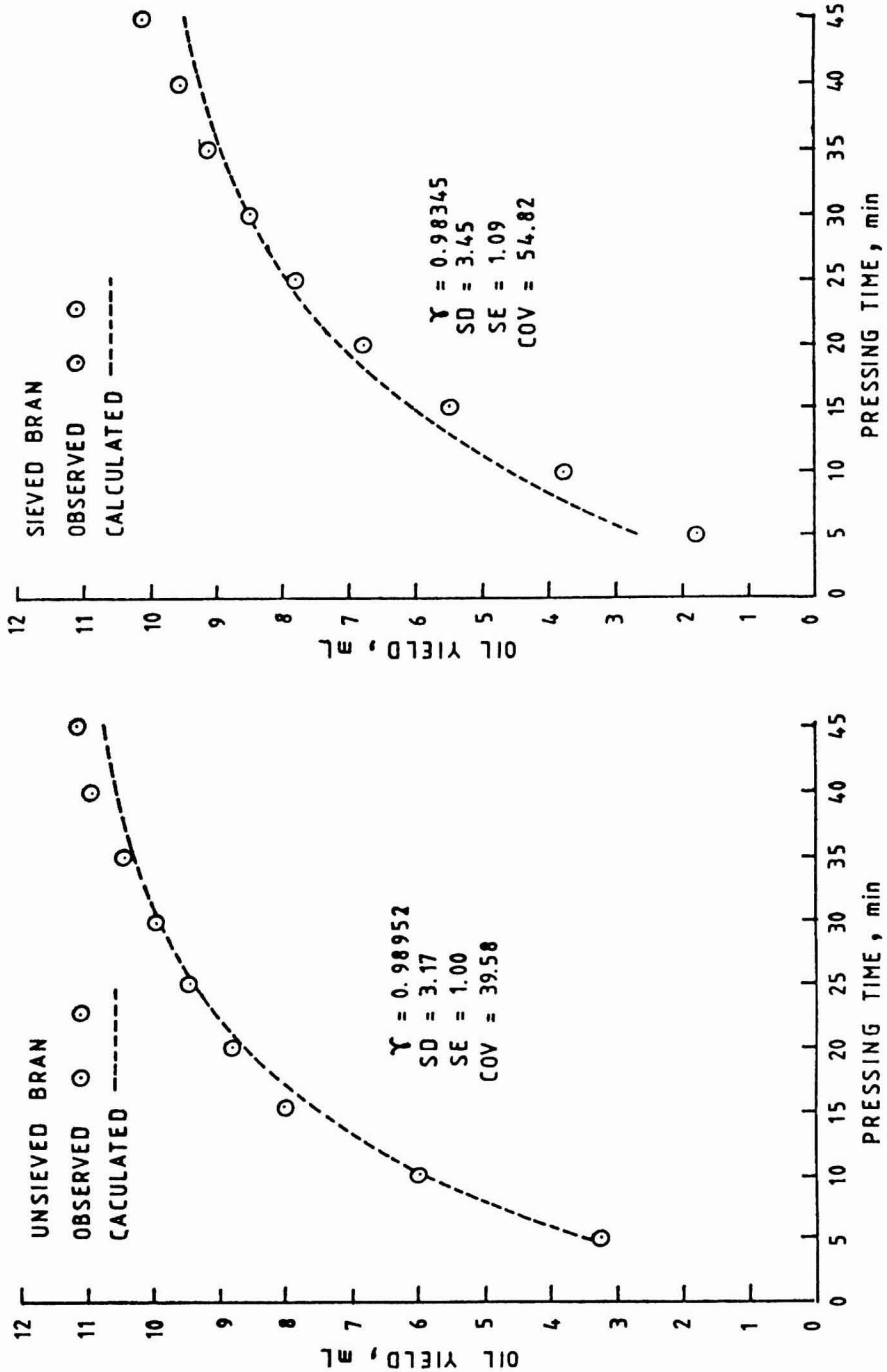

FIG. 6. EFFECT OF PRESSING TIME ON OIL YIELD AT 260 kg/cm^2

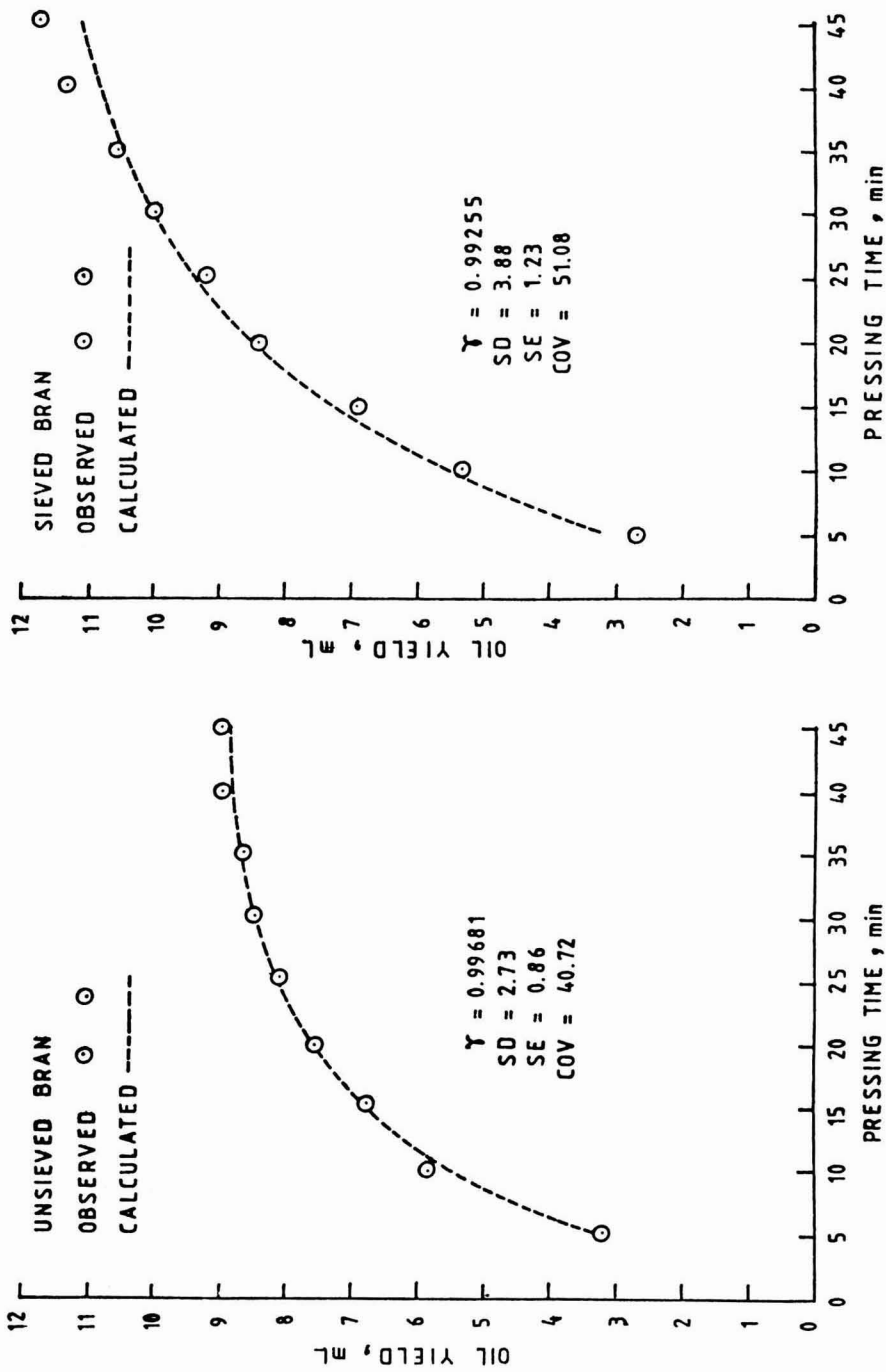

FIG. 7. EFFECT OF PRESSING TIME ON OIL YIELD AT 307.74 kg/cm^2

nature of variation of Q(obs) and Q(cal) is same at all the applied pressures, the oil yields increasing with the increase in pressing time reaching the maximum values in about 45 min.

The results indicate that there was a close agreement between calculated and observed value of oil yield with correlation coefficients (r), varying from 0.9397 to 0.9968. The closeness of the predicted values to those observed indicates that the mathematical model proposed and the constants obtained can be used for predicting oil yield of bran in the expression process.

The severity of settling of bran particles is lessened by presence of husk particles (18%). Hence, a certain degree of porosity is being maintained. Therefore, the oil yields obtained at 190 and 260 Kg/cm^2 are more in the case of unsieved bran. This indicates that the flow channels are made available continuously during the period of compression. Whereas, in the case of sieved bran, at lower pressures (72.3 and 120 kg/cm^2) the initial oil yields are more because the bran is enriched with oil content by separating husk particles. Moreover, the rearrangement of bran particles might be taking place at a faster rate in the interstices due to smaller size of the particles. Thus channels once created are sealed and further flow of oil is stopped at higher pressures. If the particles are bending or slipping one over the other, then certainly deformation cannot take place and release of oil bodies would be difficult.

REFERENCES

GURNHAM, F. C. and MASSON, H. J. 1946. Expression of liquids from fibrous materials J. Ind. Eng. Chem. *38* (12), 1309–1315.

McCABE, W. L. and SMITH, J. C. 1967. *Unit Operations of Chemical Engineering*, 2nd ed. pp. 792–808, McGraw-Hill Book Inc., New York.

MREMA, G. C. and McNULTY, P. B. 1985. Mathematical model of mechanical oil expression from oilseeds. J. Agric. Eng. Res. *31*(5), 361–370.

MURTHY, V.N.S. 1984. Compressibility and consolidation: In *Soil Mechanics and Foundation Engineering*, pp. 230–283, Dhanpat Rai and Sons, New Delhi.

PUNMIA, B. C. 1983. One dimensional consolidation. In *Soil Mechanics and Foundations*, 8th ed. pp. 337–377, Standard Book House, Delhi.

SCHARTZBERG, H. G., ABULARCH, V. and ZAMAN, S. 1982. Force requirements for water and juice expression from cellular food materials. Agricultural Experiment Station, Massachusetts, paper No. 2301, pp. 1–4.

SCHWARTZBERG, H. G., ROSENAU, J. R. and RICHARDSON, G. 1977. The removal of water by expression. In *Water Removal Processes*. (C. J. King and J. P. Clark, eds.). AICHE Symposium Series, *73* (163), 177–189.

SHIRATO, M. MURASE, T., NEGAWA, M. and SENDA, T. 1970. Fundamental studies of expression under variable pressure, J. Chem. Eng. Japan *3*(1), 106, (cited in Schwartzberg *et al.* 1977).

SINGH, J. and SINGH, B.P.N. 1987. Development of a mathematical model for oil expression process under uniaxial compression. XXIII Annual convention ISAE. J.N.K.V.V. Jabalpur, March, 9–11.

SIVALA, K. 1989. Studies on Rice Bran Oil Expression. Unpublished Ph.D. thesis, Post Harvest Technology Centre, I.I.T., Kharagpur.

TERZAGHI, K. 1943. Theory of consolidation. In *Theoretical Soil Mechanics*, 11th ed. pp. 265–296, John Wiley & Sons, New York.

BREAKAGE SUSCEPTIBILITY OF SHELLED CORN DUE TO REHYDRATION AND REDRYING

L. G. TABIL, A. NOOMHORM and L. R. VERMA

Division of Agricultural and Food Engineering
Asian Institute of Technology
Bangkok, Thailand

ABSTRACT

Processing activities such as drying expose grains to temperature and moisture gradients resulting to increased susceptibility of corn breakage. The effect of rehydration and redrying rates on the breakage susceptibility of corn was compared and evaluated. Dried corn samples were rehydrated and redried artificially. Breakage susceptibility of the samples were tested using a food grinder (blender) and Instron testing machine. Treatments consisting of a cycle of rehydration and redrying represented different rates of moisture sorption. Initial sample moisture, rehydration methods and redrying temperatures were used in comparing breakage susceptibility.

Samples of low initial moisture had higher breakage susceptibility as compared to higher initial moisture samples. The rehydration method representing the highest moisture adsorption rate resulted to samples which were more susceptible to breakage than the two rehydration methods representing intermediate and slow rates of moisture adsorption. Temperature of redrying also showed significant effects with high temperatures (80°C) resulting to grains with higher breakage susceptibility compared to samples redried with unheated air (30°C). Breakage susceptibility increased when samples were rehydrated and increased much more when they were redried.

INTRODUCTION

Low moisture corn adsorbs moisture during handling and storage to be in equilibrium with the atmosphere. These activities as well as drying expose the grain to temperature and moisture gradients. These gradients may cause expansion and contraction resulting in internal stresses (Fortes and Okos 1980). Temperature and moisture gradients in turn affect the breakage susceptibility of corn. Forces involved in handling, storage and processing cause the seed to fragment

Journal of Food Process Engineering **14** (1991) 69–82.

and increase the proportion of dust and broken kernels, resulting to added cost and labor for the removal of dust and broken kernels. Products from dry milling of this corn are less desirable because of the resulting low yield of intact endosperm and large and premium grits.

Increased breakage susceptibility is directly related to increased stress cracks in corn. Thompson and Foster (1963) reported that as the number of stress cracks in the corn kernel increased, the susceptibility to breakage increased. This phenomenon of stress cracks had been reported by Thompson and Foster (1963), Brekke (1967, 1968), Brekke and Kwolek (1969), Ekstrom *et al.* (1966) and Foster (1975).

According to Foster (1975), brittleness manifested in stress cracks caused by rapid drying is the most prevalent effect in artificially dried corn. Thompson and Foster (1963) found that artificially dried corn is more susceptible to stress cracks and breakage than those dried at lower temperature or with unheated air. Furthermore, they reported that stress crack formation was observed while grain was being dried with heated air or soon thereafter during cooling.

Stress crack formation was reported by White *et al.* (1982), resulting from the rehydration of popcorn. They observed in their study that the proportion of stress cracks of rehydrated popcorn was higher for grains of lower initial moisture content subjected to rapid rehydration rates. Chung *et al.* (1972) compared the sorption kinetics of sound and damaged yellow dent corn and observed that sorption rates decreased rapidly for broken corn compared to sound corn but later reversed after a certain sorption time.

Hustrulid (1962) found that remoistened corn at a slightly higher rates during the early stages than naturally moist samples. Similarly, Sokhansanj and Wasserman reported that drying rates of rehydrated grains, i.e., corn, slightly increased and concluded also that repetitive wetting-drying cycles do not alter the drying characterisation of grain. Kumar (1973) used the method of rehydrating corn by exposing the samples to high RH until they achieved the equilibrium moistures, but the study was conducted to determine the moisture distribution between the different parts of the corn kernel only.

Corn kernels are subjected to static and dynamic forces from harvest to the end-user. In an attempt to quantify breakage susceptibility of corn, several methods and equipment were developed. Static or impact testing which may involve single grains or grains in bulk were carried out to estimate the breakage characteristics of a sample of corn. Dynamic testing of individual kernels was reported by Mohsenin (1980), Srivastava *et al.* (1976), and Mensah *et al.* (1981) for impulse, impact or shear resistance. Several grinding studies of corn were conducted by Jindal *et al.* (1979), Pomeranz *et al.* (1986a, 1986b), and Watson and Herum (1986). While commercial breakage testers give the average breakage resistance of randomly impacted corn kernels, Jindal *et al.* (1979) suggested the use of a small rigid hammer mill where the concept of specific breakage rates

was applied as reported by Austin and Klimpel (1974, cited by Jindal *et al.* 1979). Specific breakage rate represents the resistance of a material under given conditions which is similar to mechanical properties such as modulus of elasticity determined under quasi-static and impact conditions (Jindal 1975, cited by Jindal *et al.* 1979).

The stress-strain or force-deformation relationship is the most meaningful measurement of the mechanical properties of a material (Gunasekaran and Paulsen 1985). Mechanical properties of corn are important indicators of how the kernels respond to the external forces involved during different post-harvest operations. Tempering is important in the commercial dry milling of corn where moisture of corn is usually increased to 18% or above. Shelef and Mohsenin (1969) determined the linear load limit, apparent modulus of elasticity and the modulus of deformability of shelled corn under uniaxial static conditions considering the kernel moisture. This uniaxial compression test involved testing individual kernels germ side down and using a specified loading device in the Instron testing machine.

There is a need to study the effects of rehydration and subsequent drying on the breakage susceptibility of corn, since remoistened corn is usually redried to meet the desired moisture for processing and marketing. It is not uncommon to find remoistened grains in some areas where adequate and modern storage facilities are absent. Proper storage and handling practices of corn are still needed to ensure the quality of the commodity for dry milling and to be competitive in the export market, where grading standards are strictly followed.

OBJECTIVES

The objectives of this study were:

(1) to determine the breakage susceptibility of rehydrated and redried corn by static test on single kernels and by impact test on kernels in bulk;
(2) to compare the effect of different rehydration and redrying rates on the breakage susceptibility of corn and;
(3) to determine the relationship between the measured parameters and the factors such as initial grain moisture, grain moisture upon testing, redrying temperature and others.

PROCEDURE

Sample Preparation

Shelled and air dried yellow dent corn-Suwan 1 variety, was procured from the National Corn and Sorghum Research Center of Thailand. The lot was divided

into 3 portions. One portion was shade dried for two days to 8.4%, another portion was exposed in an environment of 65% ± 2 RH for 5 days which achieved moisture content of 12.8%, and the third portion was treated and remained at the moisture content of 10%. The samples were thoroughly cleaned, sieved in 6.3 mm. mesh to remove smaller grains and foreign materials. The samples were packed in 5 kg samples in plastic bags and stored at 5°C. Prior to any storage for at least 24 h and placed at room temperature for thermal equilibration.

Rehydration

Samples were rehydrated by using air of high relative humidity in a reconditioning unit (Hsu Hui Chemical Co.). The temperature was made constant at 28°C to simulate the average ambient air temperature in many tropical areas. The temperature and the desired relative humidity were monitored using 400D Relative Humidity/Temperature Indicator (General Eastern Corp.), which was calibrated for temperature and relative humidity. Three initial sample moisture content which were 12.8, 10.0 and 8.4% were used. Wire mesh trays measuring 20 × 7 × 4 cm were used to load 100–120 g of the samples. Rehydration was accomplished in 3 methods as follows: (1) method A—samples were exposed directly to 95% ± 2 RH air, (2) method B—samples were first exposed to 75/% ± 2 RH air, and 95% ± 2 RH air was later used, and (3) method C—samples were exposed initially to air with relative humidity of 65% ± 2 and increased by 10% until 95% ± 2. The change in relative humidity was accomplished once the sample had achieved the equilibrium moisture at each RH interval.

Redrying

Rehydrated samples were dried in an air oven (Hsu Hui Chemical Corp.). The airflow was measured to be 0.60 m^3/min which was constant rate and the samples were loaded at 100–110 g unto wire mesh trays similar to those used for rehydration. The drying temperatures used were 80°C, 55°C, and 30°C. Air relative humidity at 80°C was measured to be at 2% and 17% at 55°C. The unheated air drying was conducted by maintaining the air temperature at 30°C ± 2 and relative humidity at 30% ± 3.

Grain Sampling and Moisture Determination

Sampling of the grain at different moistures in the moisture range of 8.4 and 17.9% (w.b.) was undertaken to monitor the change in breakage susceptibility during rehydration and redrying. Samples of about 700 g were taken at desired moisture levels, 600 g was used for breakage test, 5–10 g was used for the

uniaxial compression test, and the remaining was used for moisture determination.

The moisture content of the grains was monitored by keeping 5 separate loaded trays in the reconditioning unit. The change in weight at a certain time interval was taken, which indicated how much moisture the sample had adsorbed.

Uniaxial Compression Test

Selected kernels were slightly sanded in the germ side to remove the creases and the opposite side was surface ground to conform to a uniform thickness of 3.5 mm. The 20 kernels were mounted germ side down on a rigid plate using DURO EPOXE glue (Woodhill Permatex). An hour after mounting, the kernels were tested in the Instron Food Testing Instrument—Table Model 1140. The loading device used was the spherical indenter with a diameter of 1.7 mm. A compression load cell (Type 2512-206) with full scale ranges of 5, 10, 20, and 50 kg was used in testing the kernels, chart speed was set at 500 mm/min and the cross head speed at 5 mm/min. The load was set full scale at 50 kg for low moisture kernels—10% and below, and 20 kg for kernels with moisture of more than 10%. The following moisture dependent parameters were determined: the linear load limit up to which the force-deformation relationship is linear, and the apparent modulus of elasticity (Mohsenin 1970). The force-deformation curve thus obtained could not be represented in the form of a stress-strain diagram since the stresses and strains are not known. The modulus of elasticity was represented as an apparent modulus of elasticity based on the assumptions and equations in the Hertz theory.

Mechanical breakage Test by Grinding

Samples of 50 g each passing through 9.5 mm round hole and retained on 6.3 mm sieves were ground in a food blender (Moulinex, fitted with Type 241 blades) at a speed of 2300 rpm. Three grinding durations -1, 2, 3 s were used to account for the effect of impact duration, sieve size, moisture content, and the mode of rehydration treatment on the breakage resistance of the samples. The samples were sieved in U.S. standard square mesh sieves with sizes 6.3 mm, 4.75 mm, 3.35 mm, 2.36 mm, and 1.19 mm. Shaking of the sieves was accomplished by using a sieve shaker (Central Scientific), running for at least 3 minutes. The logarithmic value of the portion of total sample weight retained on a certain sieve size against the impact duration was plotted. The specific breakage rate in s^{-1} of the ground material, for a given sieve size, specific size range, and constant grinder rotation was obtained. The test was replicated four times for each grinding duration.

Statistical Analysis

Statistical Analysis System (SAS-Statistics) package (SAS Institute, Cary, N.C., U.S.A.) was used to analyze the data by analysis of variance and stepwise regression analysis procedures. The 3 × 3 × 4 factorial experiment was conducted in split-split plot design. The main plot factor was the initial sample moisture (3 levels), the subplot factor was the rehydration method (3 levels) and the sub-subplot factors were the redrying temperatures (3 levels) plus rehydration (1 level). Comparison of a pair of treatments was done using the Duncan's Multiple Range Test (DMRT). The stepwise regression procedure was used to develop models to express the relationship between the dependent variables—specific breakage rate and linear load limit, and the independent variables—moisture content of the grains, initial moisture content, equilibrium moisture content, sieve size, redrying temperature and the three rehydration methods represented by three dummy variables.

RESULTS AND DISCUSSIONS

Rehydration and Redrying Rates

Different rehydration and redrying rates as affected by initial grain moisture and the method of rehydration were obtained. Figure 1 shows a typical rela-

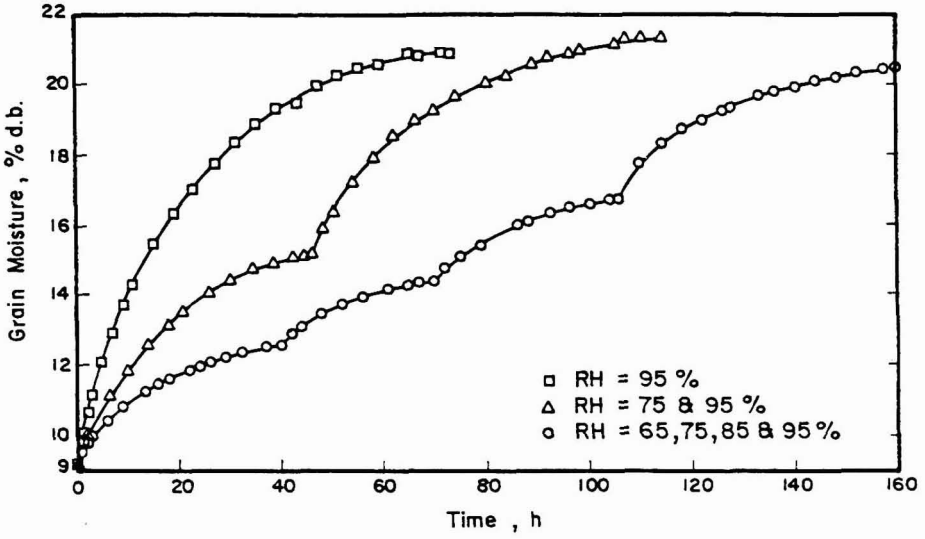

FIG. 1. MOISTURE ADSORPTION OF CORN WITH INITIAL MOISTURE OF 8.42% AT DIFFERENT REHYDRATION METHOD

tionship between exposure time and grain moisture. Method A which consist of exposing the grains to high humidity air at 95% had the highest rehydration rate, followed by methods B and C, in that order. Samples with low initial moisture did have higher moisture adsorption rate compared to samples with initial moisture of 12.8% w.b. as shown in Fig. 2.

As the rehydrated samples were redried, different drying rates were obtained. Shown in Fig. 3 is a typical drying curve at different drying air temperatures.

Mechanical Breakage Test by Grinding

Similar to the report of Jindal *et al.* (1979), the relationship between percent weight of ground material retained at a certain sieve size and the impact duration is a first-order relationship on a semilogarithmic coordinates (Fig. 4). Rehydrated samples which were redried to their previous initial moisture had higher specific breakage rates as compared to the original sample.

Using the analysis of variance (ANOVA) procedure and the Duncan's Multiple Range Test (DMRT), the effect of initial moisture content, rehydration method and redrying temperatures on specific breakage rate was evaluated. Specific breakage rate of samples subjected to rehydration and redrying treatment with an initial moisture content (IMC) of 8.4% were the highest. It was followed by samples with IMC of 10%, and the sample with IMC of 12.8% had the lowest values of specific breakage rate.

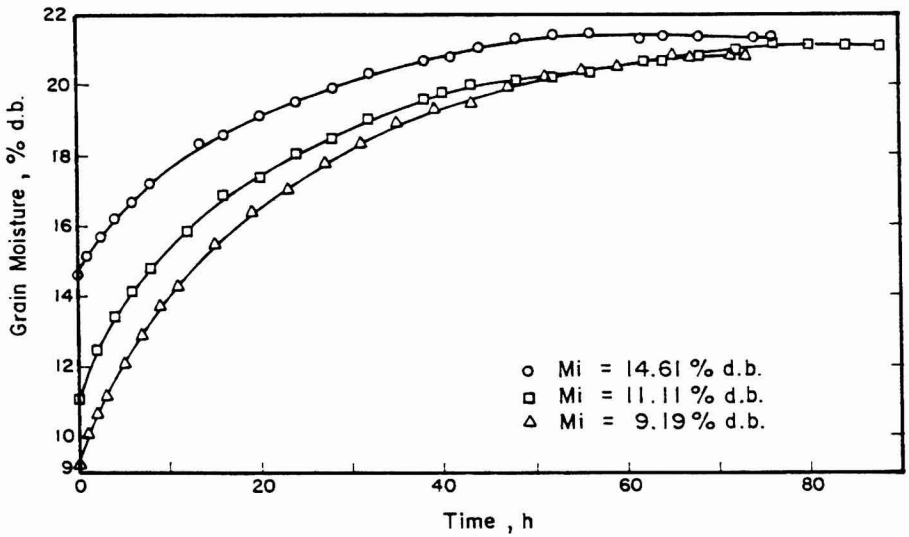

FIG. 2. MOISTURE ADSORPTION OF CORN REHYDRATED AT A RELATIVE HUMIDITY OF 95%

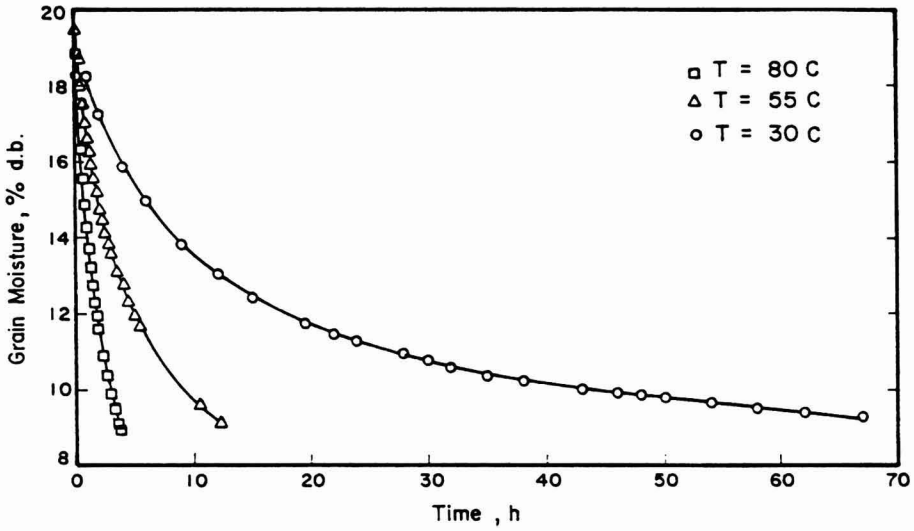

FIG. 3. DRYING OF CORN PREVIOUSLY REHYDRATED BY METHOD A AT DIFFERENT TEMPERATURE (IMC = 8.42%)

Effects of rehydration method on specific breakage rate were highly significant. In most of the samples, method A treated samples (rapid moisture adsorption rate) had the highest specific breakage rate among the three types of rehydration treatment. Method B (intermediate moisture adsorption rate) treated samples had higher specific breakage rate than method C (slow moisture adsorption rate) treated samples.

The mean specific breakage rate of the rehydrated samples was significantly lower than that of the redried samples, at all moisture levels and sieve sizes used, showing that regardless of the air temperature used in drying, specific breakage rates of the redried samples increased. Rehydrated samples dried at 80°C had the highest specific breakage rate, followed by samples dried at 55°C, and samples dried at 30°C had the lowest specific breakage rate. High drying rates as reflected by high redrying temperatures increased the breakage susceptibility of corn.

Using the MAXR method under the stepwise regression procedure of Statistical Analysis System (SAS) factor such as sieve size, grain moisture at the time of testing, drying air temperature, initial moisture content and rehydration methods were included to find the appropriate model to express specific breakage rate as a function of these factors. Since it was inappropriate to quantify the independent variable-rehydration method which the air temperature was constant at 28°C, dummy variables were included. Dummy variable was 1 for three methods of rehydration otherwise, it was zero for redried samples.

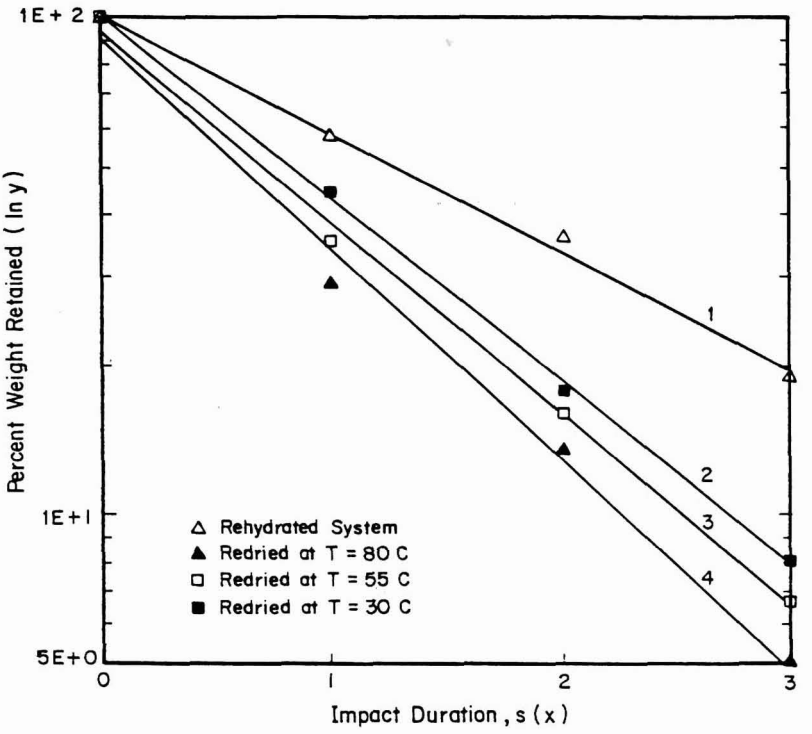

FIG. 4. A TYPICAL RELATIONSHIP BETWEEN PERCENTAGE WEIGHT RETAINED AT DIFFERENT SIEVE OPENING AND IMPACT DURATION OF CORN
(Initial Moisture Content = 10%, Rehydrated by Method A)
Line 1 In y = 2.002 − 0.2373 × ; R^2 = 0.92
Line 2 In y = 1.958 − 0.4244 × ; R^2 = 0.94
Line 3 In y = 1.975 − 0.3873 × ; R^2 = 0.95
Line 4 In y = 2.002 − 0.3662 × ; R^2 = 0.95

The specific breakage rate, k, of the sample is given as:

$$k = 0.2389 + 0.07727\ \mathrm{Ln}(M) - 0.001187\ \exp(S) + 0.00287\ S^3 + 0.19542\ S^2/M + 0.00026171\ D\ T\ S \quad (1)$$

where k = specific breakage rate, S^{-1}
M = moisture content of the sample, % d.b.
S = sieve opening, mm
T = drying air temperature, °C
D_1 = dummy variable, 1 for redried samples and 0 for rehydrated samples.

The model was highly significant at 1%, with a coefficient of determination of 0.96. Comparison of experimental value and predicted model is shown in Fig. 6.

Uniaxial Compression Test

The force-deformation relationship of each kernel tested was evaluated and a high variability of the parameters was observed. This could be due to: (a) variation in kernel size, shape and thickness, (b) variation in kernel moisture, (c) variation in texture and hardness which may exist from kernel to kernel, (d) thickness of horny endosperm, and (e) the degree of graining performed on the kernel to conform to a uniform thickness of 3.5 mm. The coefficient of variation (cv) from the linear load limit ranged from 7.6 to 34.6%, and that of the apparent modulus of elasticity from 9.4 to 34.6%. A typical force-deformation diagram is shown in Fig. 5. Linear load limit values were further analyzed by ANOVA to see if they were in agreement with the findings of the breakage test.

ANOVA results showed that at all levels of moisture, the main effects—initial moisture content, rehydration method and redrying temperature were significant at 5% level. Although initial moisture content effects were significant in com-

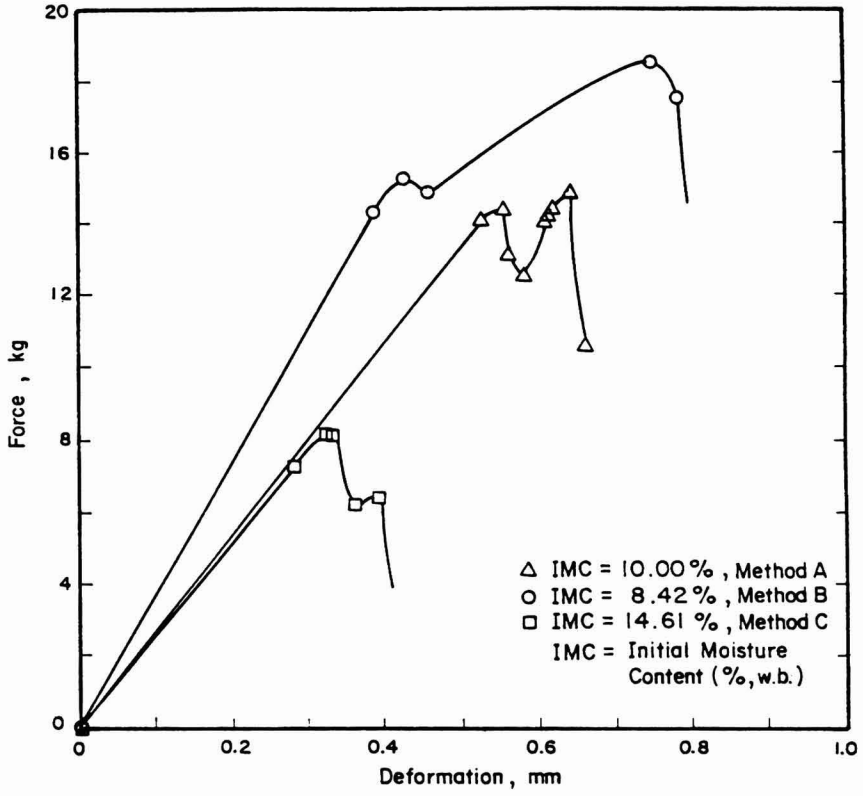

FIG. 5. A TYPICAL FORCE-DEFORMATION DIAGRAM OF REHYDRATED CORN SAMPLE

paring mean values for linear load limit, the order or arrangement as to which sample having such initial moisture had the highest and lowest mean value was not well defined in the range of grain moisture levels in which the comparison was performed.

Samples subjected to rehydration method A had the lowest mean value of linear load limit, followed by samples rehydrated by method B. Samples subjected to low rehydration rate (method C) had the highest linear load limit. High rehydration rates resulted to increased breakage susceptibility.

Linear load limit of rehydrated samples was higher than the redried samples. Redrying of the rehydrated samples at 80°C resulted in samples with very low linear load limit. Samples redried with unheated air at 30°C had the highest linear load limit. As with the specific breakage rate, high drying rates as reflected by the drying air temperatures decreased the linear load limit of corn.

A model to express the relationship of linear load limit LL (N) as a function of grain moisture M (%, w.b.), and redrying air temperature T (°C) was developed using the MAXR method under the Stepwise regression procedure of SAS which the same procedure as the Eq. 1 because of the air temperature was constant for rehydration and presented as follows:

(a) for redried samples

$$LL_1 = \exp [(60.6596 + 3.9529T)/(M + T)] \quad (2)$$

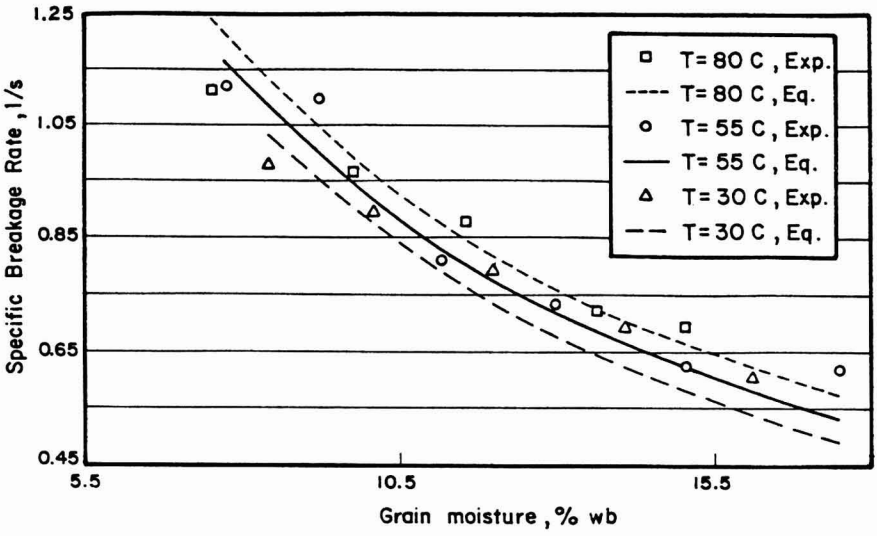

FIG. 6. COMPARISON OF EXPERIMENTAL VALUE AND PREDICTED SPECIFIC BREAKAGE RATE MODEL, FOR 6.3 MM SIEVE ON REDRIED CORN WITH INITIAL MOISTURE CONTENT OF 8.42%

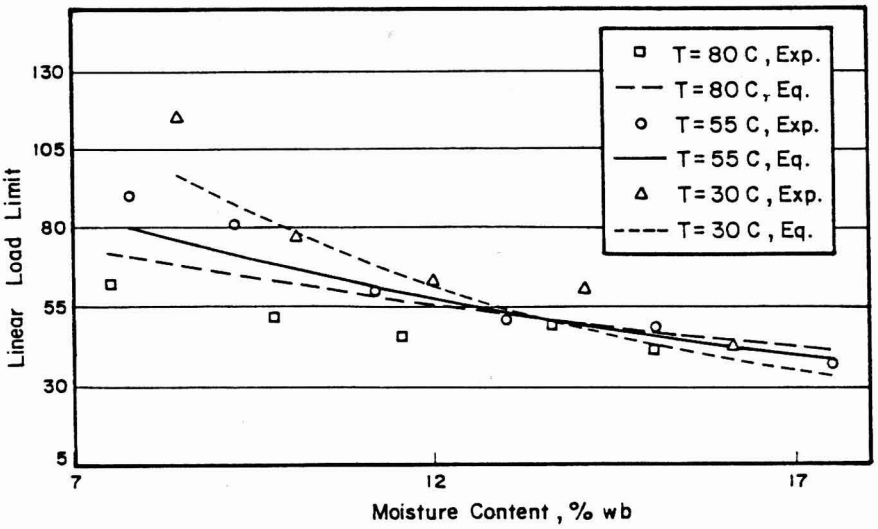

FIG. 7. COMPARISON OF EXPERIMENTAL VALUE AND PREDICTED LINEAR LOAD LIMIT MODEL, FOR 6.3 MM SIEVE ON REDRIED CORN WITH INITIAL MOISTURE CONTENT OF 8.42%

(b) for rehydrated samples

$$LL_2 = \exp [60.6596/M] \quad (3)$$

The model was highly significant at 1% with a coefficient of determination of 0.99. Comparison of experimental value and predicted model is shown in Fig. 7.

In the comparison of redried and rehydrated samples, both tests indicated that breakage susceptibility increased as the samples were redried. Comparison of means of different redrying temperatures showed that both tests consistently indicated that rehydrated and subsequently dried samples increased the breakage susceptibility of corn, depending on the drying rate as indicated by the drying temperature used. Rapid moisture removal and high temperatures cause brittleness and stress crack formation in the redried grain kernels.

SUMMARY OF RESULTS

The following summarizes the findings of the study:

(1) Specific breakage rate increased as the initial moisture content was decreased for both the rehydrated and redried samples.
(2) Linear load limit of samples, the point up to which the load-deformation

relationship is linear decreased as the rate of moisture adsorption during rehydration increased.

(3) Redrying air temperature was directly related to specific breakage rate, but inversely related to the linear load limit, indicating an increased susceptibility to breakage as drying air temperature was increased.

(4) Samples increased their susceptibility to breakage after a cycle of rehydration and redrying.

(5) Although initial moisture content effects were significant in comparing mean values of linear load limit, the relationship between latter and the initial sample moisture content was not well established.

(6) Effects of rehydration method on specific breakage rate of the samples were significant. However, the method yielding the highest or lowest specific breakage rate was not consistent in all moisture levels to which the comparison was conducted.

REFERENCES

BREKKE, O. L. 1967. Corn dry milling: pretempering low moisture corn. Cereal Chem. *44*, 521–531.

BREKKE, O. L. 1968. Corn dry millings stress crack formation in tempering of low-moisture corn, and effect on degerminator performance. Cereal Chem. *45*, 291–303.

BREKKE, O. L. and KWOLEK, W. F. 1969. Corn dry milling: cold tempering and degerming of corn of various initial moisture contents. Cereal Chem. *46*, 545–559.

CHUNG, D. S., PARK, S., HOOVER, W. J. and WATSON, C. A. 1972. Sorption Kinetics of Water Vapor by Yellow Dent Corn II. Analysis of Kinetic Data for Corn. Cereal Chem. *49*, 598–604.

EKSTROM, G. A., LIJEDAHL, J. B. and PEART, R. M. 1966. Thermal expansion and tensile properties of corn kernels and their relationship to cracking during drying. Trans. ASAE, *9*(4), 556–561.

FORTES, M. and OKOS, M. R. 1980. Changes in physical properties of corn during drying. Trans. ASAE, *23*(4), 1004–1008.

FOSTER, G. H. 1975. *Causes and Cures of Physical Damage to Corn*. Corn quality in world markets, pp. 221–229, Interstate Printers and Publishers, IL.

GUNASEKARAN, S. and PAULSEN, M. R. 1985. Breakage resistance of corn as a function of drying rates. Trans. ASAE, *28*(6), 2071–2076.

HUSTRULID, A. 1962. Comparative Drying Rates of Naturally Moist, Remoistened, and Frozen Shelled Corn. Trans. ASAE, *5*, 64–67.

JINDAL, V. K., HERUM, F. L. and HAMDY, M. Y. 1979. Selected breakage characteristics of corn. Trans. ASAE, *22*(5), 1193–1196.

KUMAR, M. 1973. Moisture Distribution Between Whole Corn, Endosperm and Germ by various Initial Moisture Contents. Cereal Chem. *46*, 545–559.

MENSAH, J. K., HERUM, F. L ., BLAISDELL, J. L. and STEVENS, K. K. 1981. Effect of drying conditions on impact shear resistance of selected corn varieties. Trans. ASAE *24*, 1568–1572.

MENSAH, J. K., HERUM, F. L. and STEVENS, K. K. 1976. Impact parameters related to physical damage to corn kernel. Trans. ASAE, *19*(6), 1147–1151.

MOHSENIN, N. N. 1980. *Physical Properties of Plant and Animal Materials*. Gordon and Breach Science Publishers, New York.

POMERANZ, Y., CZUCHAJOWSKA, Z. and LAI, F. S. 1986. Comparison of methods for determination of hardness and breakage susceptibility of commercially dried corn. Cereal Chem. *63*, 39–42.

POMERANZ, Y., HALL, G. E., CZUCHAJOWSKA, Z. and LAI, F. S. 1986b. Test weight, hardness, and breakage susceptibility of yellow dent corn hybrids. Cereal Chem. *63*(4), 349–351.

SHELEF, L. and MOHSENIN, N. N. 1969. Effects of moisture content on mechanical properties of corn horny endosperm. Cereal Chem. *46*, 242–253.

SOKHANSANJ, S. and WASSERMAN, J. D. 1981. Drying Characteristics of Several Grains Subjected to Repetitive Wetting and Drying Cycles. ASAE Paper No. 81-3528, Am. Soc. Agric. Eng., St. Joseph, MI.

SRIVASTAVA, A. K., HERUM, F. L. and STEVENS, K. K. 1976. Impact parameters related to physical damage to corn kernel. Trans. ASAE, *19*(6), 1147–1151.

THOMPSON, R. A. and FOSTER, G. H. 1963. Stress cracks and breakage in artificially dried corn. Marketing Research Bulletin, No. 631, TFRD, AMS, USDA.

WATSON, S. A. and HERUM, F. L. 1986. Comparison of eight devices for measuring breakage susceptibility of shelled corn. Cereal Chem. *63*, 139–142.

WHITE, G. M., ROSS, I. J. and PONELEIT, G. G. 1982. Stress crack development in popcorn as influenced by drying and rehydration processes. Trans. ASAE, *25*(3), 768–772.

ERRATA Corrected 22 7034

In *J. of Food Process Engineering* Vol. 13, No. 3 Artic. 1 "Particle/Fluid Interface Heat Transfer Under UHT Conditions at Low Particle/Fluid Relative Velocities" by D. I. CHANDARANA, A. GAVIN, III and F. W. WHEATON, two errors were found.

On p. 200 Eq. 6 reads $Nu = 2.0 + 2.82 \times 10^{-2}Re^{1.6}Pr^{0.89}$
The correct Eq. 6 is $Nu = 2.0 + 2.82 \times 10^{-3}\ Re^{1.16}Pr^{0.89}$

On p. 201 Eq. 7 reads $Nu = 2.0 + 3.33 \times 10^{-2}\ Re^{1.08}$
The correct Eq. 7 is $Nu = 2.0 + 1.33 \times 10^{-3}\ Re^{1.08}$

Journal of Food Process Engineering **14** (1991) 83.

F
N
P

PUBLICATIONS IN FOOD SCIENCE AND NUTRITION

Journals

JOURNAL OF MUSCLE FOODS, N.G. Marriott and G.J. Flick, Jr.
JOURNAL OF SENSORY STUDIES, M.C. Gacula, Jr.
JOURNAL OF FOOD SERVICE SYSTEMS, O.P. Snyder, Jr.
JOURNAL OF FOOD BIOCHEMISTRY, J.R. Whitaker, N.F. Haard and H. Swaisgood
JOURNAL OF FOOD PROCESS ENGINEERING, D.R. Heldman and R.P. Singh
JOURNAL OF FOOD PROCESSING AND PRESERVATION, D.B. Lund
JOURNAL OF FOOD QUALITY, R.L. Shewfelt
JOURNAL OF FOOD SAFETY, T.J. Montville and A.J. Miller
JOURNAL OF TEXTURE STUDIES, M.C. Bourne and P. Sherman

Books

NUTRIENT ADDITIONS TO FOOD, J.C. Bauernfeind and P.A. Lachance
NITRITE-CURED MEAT, R.G. Cassens
THE POTENTIAL FOR NUTRITIONAL MODULATION OF THE AGING PROCESSES, D.K. Ingram *et al.*
CONTROLLED/MODIFIED ATMOSPHERE/VACUUM PACKAGING OF FOODS, A.L. Brody
NUTRITIONAL STATUS ASSESSMENT OF THE INDIVIDUAL, G.E. Livingston
QUALITY ASSURANCE OF FOODS, J.E. Stauffer
THE SCIENCE OF MEAT AND MEAT PRODUCTS, 3RD ED., J.F. Price and B.S. Schweigert
HANDBOOK OF FOOD COLORANT PATENTS, F.J. Francis
ROLE OF CHEMISTRY IN THE QUALITY OF PROCESSED FOODS, O.R. Fennema, W.H. Chang and C.Y. Lii
NEW DIRECTIONS FOR PRODUCT TESTING AND SENSORY ANALYSIS OF FOODS, H.R. Moskowitz
PRODUCT TESTING AND SENSORY EVALUATION OF FOODS, H.R. Moskowitz
ENVIRONMENTAL ASPECTS OF CANCER: ROLE OF MACRO AND MICRO COMPONENTS OF FOODS, E.L. Wynder *et al.*
FOOD PRODUCT DEVELOPMENT IN IMPLEMENTING DIETARY GUIDELINES, G.E. Livingston, R.J. Moshy, and C.M. Chang
SHELF-LIFE DATING OF FOODS, T.P. Labuza
RECENT ADVANCES IN OBESITY RESEARCH, VOL. V, E. Berry *et al.*
RECENT ADVANCES IN OBESITY RESEARCH, VOL. IV, J. Hirsch *et al.*
RECENT ADVANCES IN OBESITY RESEARCH, VOL. III, P. Bjorntorp *et al.*
RECENT ADVANCES IN OBESITY RESEARCH, VOL. II, G.A. Bray
RECENT ADVANCES IN OBESITY RESEARCH, VOL. I, A.N. Howard
ANTINUTRIENTS AND NATURAL TOXICANTS IN FOOD, R.L. Ory
UTILIZATION OF PROTEIN RESOURCES, D.W. Stanley *et al.*
VITAMIN B_6: METABOLISM AND ROLE IN GROWTH, G.P. Tryfiates
FOOD POISONING AND FOOD HYGIENE, 4TH ED., B.C. Hobbs *et al.*
POSTHARVEST BIOLOGY AND BIOTECHNOLOGY, H.O. Hultin and M. Milner

Newsletters

MICROWAVES AND FOOD, R.V. Decareau
FOOD INDUSTRY REPORT, G.C. Melson
FOOD, NUTRITION AND HEALTH, P.A. Lachance and M.C. Fisher
FOOD PACKAGING AND LABELING, S. Sacharow

GUIDE FOR AUTHORS

Typewritten manuscripts in triplicate should be submitted to the editorial office. The typing should be double-spaced throughout with one-inch margins on all sides.

Page one should contain: the title, which should be concise and informative; the complete name(s) of the author(s); affiliation of the author(s); a running title of 40 characters or less; and the name and mail address to whom correspondence should be sent.

Page two should contain an abstract of not more than 150 words. This abstract should be intelligible by itself.

The main text should begin on page three and will ordinarily have the following arrangement:

Introduction: This should be brief and state the reason for the work in relation to the field. It should indicate what new contribution is made by the work described.

Materials and Methods: Enough information should be provided to allow other investigators to repeat the work. Avoid repeating the details of procedures which have already been published elsewhere.

Results: The results should be presented as concisely as possible. Do not use tables *and* figures for presentation of the same data.

Discussion: The discussion section should be used for the interpretation of results. The results should not be repeated.

In some cases it might be desirable to combine results and discussion sections.

References: References should be given in the text by the surname of the authors and the year. *Et al.* should be used in the text when there are more than two authors. All authors should be given in the Reference section. In the Reference section the references should be listed alphabetically. See below for style to be used.

DEWALD, B., DULANEY, J.T., and TOUSTER, O. 1974. Solubilization and polyacrylamide gel electrophoresis of membrane enzymes with detergents. In *Methods in Enzymology,* Vol. xxxii, (S. Fleischer and L. Packer, eds.) pp. 82–91, Academic Press, New York.

HASSON, E.P. and LATIES, G.G. 1976. Separation and characterization of potato lipid acylhydrolases. Plant Physiol. *57,*142–147.

ZABORSKY, O. 1973. *Immobilized Enzymes,* pp. 28–46, CRC Press, Cleveland, Ohio.

Journal abbreviations should follow those used in *Chemical Abstracts.* Responsibility for the accuracy of citations rests entirely with the author(s). References to papers in press should indicate the name of the journal and should only be used for papers that have been accepted for publication. Submitted papers should be referred to by such terms as "unpublished observations" or "private communication." However, these last should be used only when absolutely necessary.

Tables should be numbered consecutively with Arabic numerals. The title of the table should appear as below:

Table 1. Activity of potato acyl-hydrolases on neutral lipids, galactolipids, and phospholipids

Description of experimental work or explanation of symbols should go below the table proper. Type tables neatly and correctly as tables are considered art and are not typeset. Single-space tables.

Figures should be listed in order in the text using Arabic numbers. Figure legends should be typed on a separate page. Figures and tables should be intelligible without reference to the text. Authors should indicate where the tables and figures should be placed in the text. Photographs must be supplied as glossy black and white prints. Line diagrams should be drawn with black waterproof ink on white paper or board. The lettering should be of such a size that it is easily legible after reduction. Each diagram and photograph should be clearly labeled on the reverse side with the name(s) of author(s), and title of paper. When not obvious, each photograph and diagram should be labeled on the back to show the top of the photograph or diagram.

Acknowledgments: Acknowledgments should be listed on a separate page.

Short notes will be published where the information is deemed sufficiently important to warrant rapid publication. The format for short papers may be similar to that for regular papers but more concisely written. Short notes may be of a less general nature and written principally for specialists in the particular area with which the manuscript is dealing. Manuscripts which do not meet the requirement of importance and necessity for rapid publication will, after notification of the author(s), be treated as regular papers. Regular papers may be very short.

Standard nomenclature as used in the engineering literature should be followed. Avoid laboratory jargon. If abbreviations or trade names are used, define the material or compound the first time that it is mentioned.

EDITORIAL OFFICES: DR. D.R. HELDMAN, COEDITOR, *Journal of Food Process Engineering,* National Food Processors Association, 1401 New York Avenue, N.W., Washington, D.C. 20005 USA; or DR. R.P. SINGH, COEDITOR, *Journal of Food Process Engineering,* University of California, Davis, Department of Agricultural Engineering, Davis, CA 95616 USA.

CONTENTS